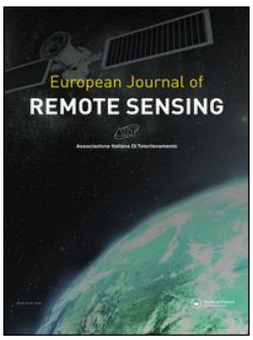

European Journal of Remote Sensing

ISSN: (Print) 2279-7254 (Online) Journal homepage: https://www.tandfonline.com/loi/tejr20

Evaluation of the influence of disturbances on forest vegetation using Landsat time series; a case study of the Low Tatras National Park

Radovan Hladky, Josef Lastovicka, Lukas Holman & Premysl Stych

To cite this article: Radovan Hladky, Josef Lastovicka, Lukas Holman & Premysl Stych (2020) Evaluation of the influence of disturbances on forest vegetation using Landsat time series; a case study of the Low Tatras National Park, European Journal of Remote Sensing, 53:1, 40-66, DOI: 10.1080/22797254.2020.1713704

To link to this article: https://doi.org/10.1080/22797254.2020.1713704

Published online: 02 Mar 2020.

EUROPEAN JOURNAL OF REMOTE SENSING
2020, VOL. 53, NO. 1, 40–66
https://doi.org/10.1080/22797254.2020.1713704

Taylor & Francis
Taylor & Francis Group

Evaluation of the influence of disturbances on forest vegetation using Landsat time series; a case study of the Low Tatras National Park

Radovan Hladky[a,b], Josef Lastovicka[a], Lukas Holman[a] and Premysl Stych[a]

[a]Department of Applied Geoinformatics and Cartography, Faculty of Science, Charles University, Prague, Czech Republic; [b]Administration of the Low Tatras National Park, State Nature Conservation of the Slovak Republic (NAPANT), Banska Bystrica, Slovakia

ABSTRACT

This study is focused on the evaluation of forest vegetation changes that took place between 1992 and 2015 in the Low Tatras National Park in Slovakia, using time series on Landsat 4, 5, 7, and 8 data. Time-series analysis was performed by evaluating the development of six vegetation indices in nine different localities selected based on the type of damage. The CDR (Climate Data Records) of the Landsat data was first normalized using the PIF method, and the trajectories of the used vegetation indices were compared with in-situ data. The area was damaged by both wind and bark beetles that significantly affected the forest vegetation in the Low Tatras National Park at the beginning of the 21st century. The results confirmed the excellent predictive abilities of vegetation indices based on SWIR bands (e.g. NDMI) for the purpose of evaluating the individual stages of a disaster. The use of the Landsat data CDR in the research of long-term forest vegetation changes is of high relevance and perspective owing to the free availability and distribution of the corrected data. Finally, several applications of remote sensing data are proposed for the management and the protection of national parks.

ARTICLE HISTORY
Received 3 March 2019
Revised 5 January 2020
Accepted 7 January 2020

KEYWORDS
Time series; Landsat; vegetation indices; forest disturbance; the Low Tatras; Slovakia

Introduction

Earth observation (EO) provides unique information for the purpose of observing dynamic phenomena occurring on the surface of the Earth. Because of the availability of free data via archives, including satellite imagery and processing technology, new possibilities have been made available for studying dynamic changes to the landscape (Roy et al., 2014; Wulder, Masek, Cohen, Loveland, & Woodcock, 2012). One of the most recent issues approached using EO image analysis is to determine the health of the forests and changes that have occurred in the forests on a continental or global level. One of the most significant outputs as yet is the worldwide database covering the status and changes in the forests by Hansen, Stehman, and Potapov (2010) or the database of changes in the forests of Eastern Europe by Potapov et al. (2015). The basic sources of data used in these areas of research is the Landsat Thematic Mapper, the Enhanced Thematic Mapper Plus (TM/ETM +), and more recently the Operational Land Imager (OLI).

Time Series (TS) methods are often used to evaluate changes in vegetation. The essence of TS is the representation of the dynamics of a phenomena expressed as changes in monitored values over time. The output of a graph, or a series of graphs, brings us closer to an accurate understanding of specific phenomena using the trajectory in a line graph. TS technologies are widely used not only in the field of EO and geoinformatics, but have been used in many other scientific disciplines as well (for example biology, see Jakobsen, Carstensen, Harrison, & Zingone, 2015). EO data is mainly applied for investigating Land Cover/Land Use, understanding the current state of vegetation (Forkel et al., 2013), or in the study and observation of changes in arid, semiarid, or glacial areas (Baumann, 2011).

Many different types of satellite data can be used for TS investigation. When choosing the type of data to be used, the availability and suitability of images are initially considered (especially in terms of time and spatial resolution). Due to the availability of the free archives, the satellite imagery from Landsat is some of the most commonly used data (Wulder et al., 2016). Neigh et al. (2014) took advantage of the Landsat data to research the development of the forests in Wisconsin and Minnesota, using an algorithm that maps any disturbances to insect populations using time series. Zhu and Woodcock (2014) used the data to systematically address changes taking place in forested areas, in North America.

Tracking the dynamics of changes in the forest vegetation of Central Europe has been undertaken by several scientists. Many studies have been carried out since 1990 to evaluate the damage that industrial emissions in the Black Triangle area (the traditional industrial area between the Czech Republic, Germany,

CONTACT Premysl Stych stych@natur.cuni.cz Department of Applied Geoinformatics and Cartography, Faculty of Science, Charles University, Prague 128 43, Czech Republic

and Poland) caused, e.g. Entcheva et al. (1999), Campbell et al. (2004), and Albrechtova and Rock Barrett (2003). A systematic investigation of the use of vegetation indices in the field of deforestation and evaluating the consequences of disturbances in Sumava National Park (in the Czech Republic) has been dealt with by Hais, Jonasova, Langhammer, and Kucera (2009a), Hais & Kucera (2009b) and (2016). Hajek and Svoboda (2007) used Landsat images to evaluate the damage that occurred in a spruce forest in Trojmezna in the Sumava National Park using a time series of aerial photographs to investigate an invasion of the bark beetle. An evaluation of the impact of catastrophic events on the state and development the forest in Sumava was also the focus of Zemek, Cudlin, Bohac, Moravec, and Herman (2003). Several studies have also been carried out using EO in Krkonose National Park and Krusne hory (in the Czech Republic) Kupkova et al. (2017), Kupkova and Potuckova (2018). Musilova (2012) used EO techniques to assess the health conditions and development of spruce stands using very high-resolution data and Landsat time series to evaluate the spruce stands while applying a broad range of vegetation indices. The result of the evaluation assessed the long-term development of the health status of the spruce stands, as well as a mutual comparison of the indicating capabilities of the vegetation indices used. An evaluation of the changes in forest vegetation in Slovakia has also been carried out in several studies, Bucha (2014), Bucha and Koreň (2017), Griffiths et al. (2014), Havasova, Bucha, Ferencik, and Jakus (2015), Hlasny et al. (2015), Kern et al. (2017), Vladovic (2011) or Hlasny and Sitkova (2010), and in Poland with a focus on the High Tatras (e.g. Kozak, 2010; Kozak, Estreguil, & Troll, 2007). The complex assessment of the changes in the forest areas and their consequences in the Carpathian region has also been addressed in several Landsat studies, such as those carried out by Kuemmerle, Hostert, Radeloff, Perzanowski, and Kruhlov (2007) and Butsic et al. (2017).

This work is focused on evaluating the changes in the forest vegetation of selected localities in the Low Tatras National Park using TS methods and based on data from Landsat images. Changes in the forest vegetation that have been caused by various disturbances are evaluated on the basis of the vegetation indices selected and from data gathered in the field. The main aim of this study is to evaluate the potential of the selected vegetation indices for providing information concerning the detection of disasters (such as high winds or bark beetle invasions) and to evaluate the health of the forest during the individual stages of a disturbance (the condition of the forest before, during, and after such events). The values gathered from the time series of the selected vegetation indices are monitored and evaluated for each individual type of disturbances (biotic and abiotic) and the individual phases (pre-disturbance, disturbance, and post-disturbance). The individual trajectories of the TS are interpreted and validated in relation with the in-situ data provided by the Administration of the Low Tatras National Park. We cooperated with the Low Tatras National Park Administration in the process of collecting and evaluating the data. For this reason, an important part of this study is an evaluation of the application of the EO data and methods for the management and protection of national parks.

The main objectives of this work are:

(1) To evaluate the changes to the forest vegetation in selected localities of the Low Tatras National Park in the period 1992–2015 using Landsat data and TS methods.
(2) To evaluate the suitability of individual vegetation indices to capture the influence of different types of biotic and abiotic disturbances on forest vegetation.
(3) To validate and interpret the results of TS using in-situ data.
(4) To discuss the application of the EO data for use in nature conservation and the management of national parks.

Description of the observed area

The Low Tatras are among the most important mountainous regions of Slovakia, represented by a massive range that crosses the center of Slovakia in an east-west direction for approximately 70 kilometers. The average width of the mountain range is 15 to 30 kilometers, with a maximum height of 2 043 meters above sea level at the summit of Dumbier.

Due to its large size, the diverse soil substrate, and the variation in the forms of relief, the Low Tatras are a part of the area with the highest diversity of plant species in Slovakia. The dominant plant community in the area is forest, with the presence of extensive forest ecosystems.

Spruce trees are found with a typical naturally occurring structure in the natural forest ecosystems, and forests which have undergone forestry applications differ significantly from the former. The natural spruces are generally preserved in the less accessible areas, with forested areas that are typically smaller than the areas of forest used for economical gain. Spruces from the economically affected areas are significantly different from the spruces of natural origin in spatial construction, and especially in terms of synecological relationships as the development of these relationships takes place under the influence of both natural and anthropogenic factors. Overall, this biotope belongs to the most extensive administratively protected habitat in Slovakia with the

highest levels of territorial protection. Mountain and alpine spruce stands have been endangered by the long-distance transmission of pollutants (acidification, ozone), and by global warming and wind calamities that have led to the introduction of sub-shell insects. The integrity of the forest ecosystems has undergone significant disturbances from abiotic events (wind, snow, frost, avalanches), biotic agents (sub-insects), and anthropogenic influences (e.g. air pollution). Forest ecosystems that are economically affected are predominantly optimum to suboptimal in terms of grading for the occurrence of the bark beetle (S-NAPANT, 2007).

The declaration of the Low Tatras National Park (hereinafter NAPANT) occurred in 1978. The national park covers an area of 73 km^2 with a buffer zone of more than 110 km^2. NAPANT is one of the largest protected areas, not only in Slovakia, but in the entire Carpathians (Figure 1).

Between 15:00 and 24:00 on 19 November 2004, a windstorm passed through the Low Tatras with a maximum speed of approximately 175 km/h. Both the Low Tatras National Park and its buffer zone was severely damaged, with the destruction of forest stands in several localities. The risk of a spontaneous invasion of sub-insects in the spruce forests could not be excluded following this storm because of the threat from the surrounding forest stands. The amount of damaged wood that had to be removed was evidence of how dramatic the disaster was. In the period leading up to 2 December 2004, 950 000 m^3 of damaged wood was recorded in the Low Tatras (NAPANT Report, 2004). A loss of 1 355 000 m^3 was recorded in 2005 in the state forest of the Low Tatras area, and 177 000 m^3 of timber was harvested by state foresters in the Low Tatras in 2006, of which 80.8% was calamity wood (Kunca, Galko, & Zubrik, 2014; S-NAPANT Report, 2008).

The windstorm in November 2004 hit the territory of NAPANT strongly and ultimately led to an invasion of the European bark beetle (Ips typographus) as a result, causing a biotic disaster beneath the bark of the trees that occurred after 2005. Extremely favorable

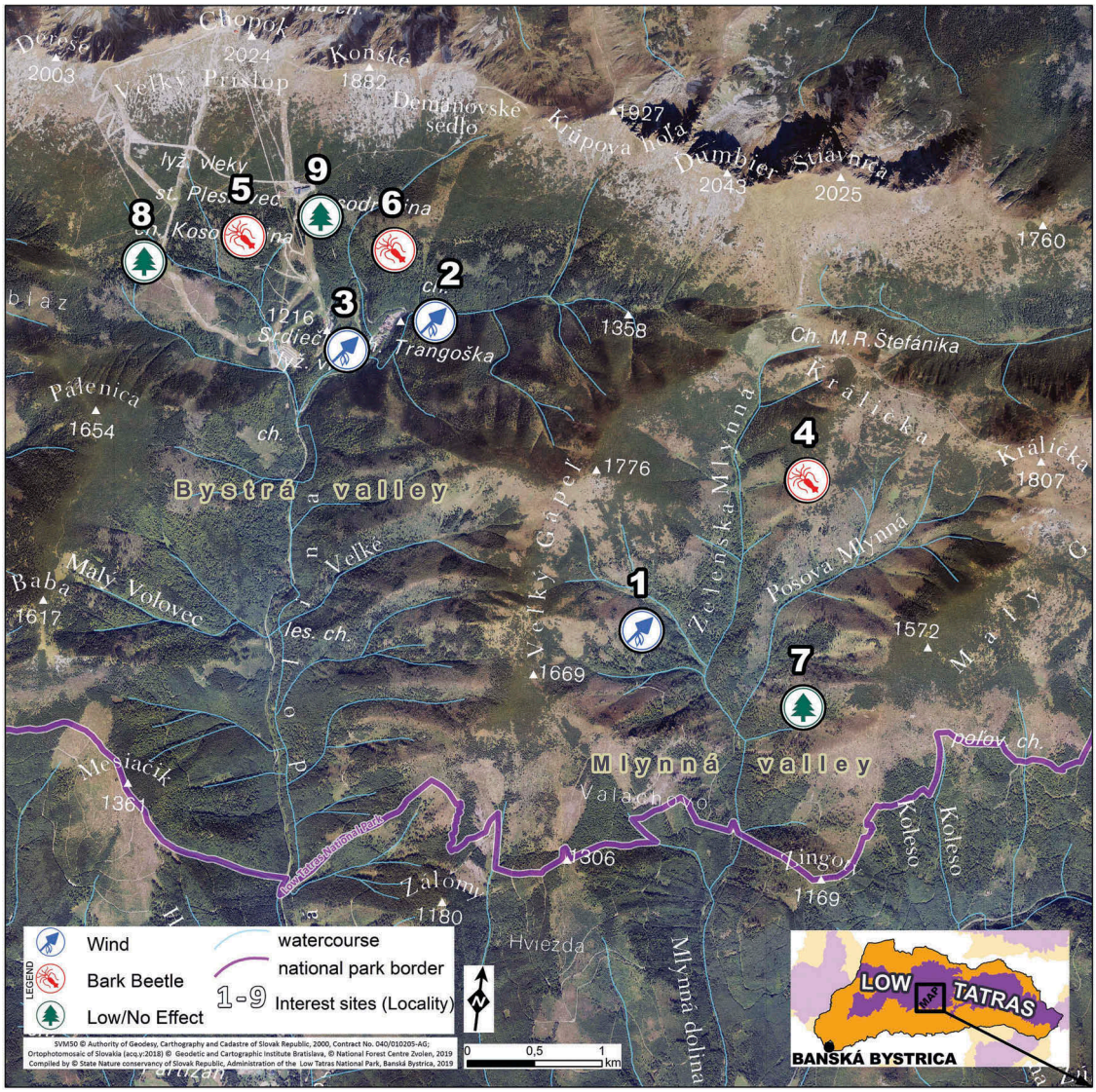

Figure 1. Map of the sites of interest (source: own creation, ESRI data).

conditions for the movement of these subcortical insects occurred in almost all of the non-native and natural spruces in Slovakia during the summer of 2007. An archived report from the National Park concerning an assessment of the current state of the insect population (S-NAPANT Report, 2008) included areas that were partially or dramatically damaged. The territory of the Low Tatras was also hit by other disasters in the following years (Kunca et al., 2014), the most important of which were the snow storm "Tamara" (in Jan. 2006), the windstorms "Kyrill" (in Jan. 2007), "Filip" (in Aug. 2007), and "Zofia" (in May 2014), and the advancing biotic calamities that have occurred in several parts of the territory.

Aspects of the changes/stability of forest areas, forestry intensity, and damage caused by the disturbances after 2004 all played a role in the selection of the sites of interest (Figure 1), which are located in the Dumbier part of the Low Tatras (Western Carpathians), the Mlynna valley, and the Bystra valley. Both valleys are part of the territory that is classified as 3rd of 5 levels of territorial protection (national park), according to the official national categorization of nature protection. The Mlynna valley is approximately 7 km long, and is divided into two by Zelenska Mlynna valley and Posova Mlynna valley. To protect this valley, Slovakia has committed to pre-accession agreements with the European Union (NATURA 2000). The territory is currently part of a site of Community importance ("SKUEV 0302 Dumbierske Tatry") and part of a special protection area ("SKCHVU 018 Nizke Tatry"). This area was originally proposed by conservationists as a strictly protected zone, but foresters did not agree. The Mlynna valley has therefore been defined as under forest management. Despite the high value of the ecosystem and the inaccessibility of the area due to the high altitudes and steep slopes (it is located 1 200–1 500 m above sea level), intensive logging has been introduced; foresters harvested approximately 268 000 m^3 of wood in this area in 2016. Only 10–30% of this wood has to be left untouched according to rules set out by the state administration authorities.

The Bystra valley is approximately 8.5 km in length. Although a busy road leading from Bystra village passes through the Bystra valley to the center of tourism in the southern side of Chopok peak, the valley itself is not a tourist destination. A primeval forest is located in this valley which has been well-preserved for centuries. The primeval forest in Bystra valley has been preserved in six areas, covering a total of almost 410 ha and in two other areas within the forest a residual primeval forest covering an area of less than 25 ha can be found. The integrity of some parts of the forest has been damaged by the cattle grazing and logging. The majority of the primeval forest is represented by Acidophilous spruce forests (*Vaccinio-Piceetea*).

In both valleys the predominant tree is the spruce (Picea abies), which occurs naturally in mountain spruce forests ecosystems. The lower foothills include beech forests (Fagus sylvatica) and mixed forests. Mountain pine (Pinus mugo) dominates above the upper boundary of the forest, together with alpine grasslands and herbaceous stands. After the windstorm in 2004, these valleys were affected by the bark beetle invasion, culminating in a decline in spruce in 2009, with a corresponding peak in the decay of the entire forest in 2012.

The sites of interest for this study were categorized according to the type of disturbance that affected these locations. The first group of sites represents the territory influenced by wind (aerial photographs and a photo of the local forest are presented in Attachments - Table 3-5 and Figure 11-16). The second group of sites has been affected by bark beetle (aerial photographs and a photo of the local forest are presented in Attachments - Table 6-8 and Figure 17-22), and the third group of sites is characterized as locations where only a very low impact of disturbance occurred in the forest (aerial photographs and a photo of the local forest are presented in Attachments - Table 9-11 and Figure 23-28).

Data

Both satellite data and in-situ data were used in this study. Landsat CDR (Climate Data Record, Landsat Collection 1 Level-2 with L1TP) satellite imageries were used as the remote sensing data. The distributed CDR data is preprocessed to include atmospheric corrections (LEDAPS algorithm for Landsat 4–7 and LaSRC for Landsat 8) using the CDR database (Vuolo, Mattiuzzi, & Atzberger, 2015). The images from Landsat 4–7 are eight-bit datasets and those from Landsat 8 are twelve-bit datasets. The Level-2 datasets are rescaled to a sixteen-bit structure to improve comparability. The CDR frames are therefore scaled to the date of the sixteen-bit structure. Other useful layers such as the Fmask (by Zhu, Wang, & Woodcock, 2015; Zhu & Woodcock, 2012) layer, which provides a mask for classified opaque elements such as water, cloud cover, snow, and shadows, can be found in the generated raster mask (from the original satellite image); for more information on the methodologies used see (Zhu et al., 2015; Zhu & Woodcock, 2014).

A total of 11 usable Landsat satellite images were finally selected covering the area of interest in this study. One Landsat 4, six Landsat 5, two Landsat 7, and two Landsat 8 images were chosen from between 1992 and 2015. An overview of all the images used is documented in Table 1. Important aspects that were considered for selection were cloud cover (elimination) and the date of acquisition. According to several authors, such as Griffiths et al. (2012) and Vogelmann,

Table 1. List of the used images (source: USGS).

Name of image	Date of acquisition	Sensor
LC81880262015193LGN00	*12 July 2015*	*Landsat 8*
LC81880262013219LGN00	*7 August 2013*	*Landsat 8*
LT51880262011198MOR00	*17 July 2011*	*Landsat 5*
LT51880262009240KIS00	*28 August 2009*	*Landsat 5*
LT51880262007203MOR00	*22 July 2007*	*Landsat 5*
LT51880262006200KIS01	*19 July 2006*	*Landsat 5*
LT51880262005245KIS00	*2 September 2005*	*Landsat 5*
LE71880262001242SGS00	*30 August 2001*	*Landsat 7*
LE71880261999221SGS01	*9 August 1999*	*Landsat 7*
LT51880261994183XXX02	*2 July 1994*	*Landsat 5*
LT41880261992202XXX02	*20 July 1992*	*Landsat 4*

Xian, Homer, and Tolk (2012), the best time for the assessment of the forest vegetation is between the summer and the autumn. Images from the months between July and September were therefore selected.

In-situ data obtained from the Low Tatras National Park include field records, information concerning forest management plans, and archived records of nature conservation documentation for the areas assessed during the study period. The forest management plan is legislatively enshrined in the Forest Law on Forest Economic Planning and is being developed as a basis for forest status and forest management for a period of 10 years. Three aspects are included in the plan; a textbook, a document detailing the economy, and maps of the forest. All the necessary data concerning the state of the forest and its management can be found in the text and the economic document. Data was provided concerning the status of the forest and the past management in the sites monitored; the area and category of forest, the age of the stock, a percentual representation of the individual trees, the average height, methods of management, and economic proposals.

The sites of interest were categorized according to the type of disturbance selected (Table 2), and were subsequently evaluated using Landsat multispectral images.

Data processing

In order to determine the state of and the changes to the vegetation from satellite images, key information is found in the spectral characteristics of the vegetation species studied. Each species of vegetation has specific characteristics that can be detected via EO, and the properties of these species (e.g. health status) can be determined based on this knowledge. Spectral reflection can be represented by a curve divided into three basic parts according to the main structural properties: the area of pigmentation absorption, cellular structures, and the amount of water absorbed (see Albrechtova & Rock Barrett, 2003). Time series analysis monitors the changes in vegetation over long periods of time, and is often used for estimating the spectral characteristics of objects studied, or is based on the spectral characteristics of derived data such as vegetation indices.

In order to ensure compatibility, the Landsat CDR data source was used. As mentioned above, atmospheric and radiometric corrections did not need to be performed on the CDR data because the images are distributed with the appropriate corrections, and are already converted to surface reflectance. The Fmask feature (Zhu et al., 2015; Zhu & Woodcock, 2012, 2014) was used to select cloud-free images and to unmask clouds, shadows, snow, and other problematic elements.

It is clear from many studies that one significant problem in creating a time series is ensuring compatibility between the types of data that are often taken with multiple types of sensors (e.g. Vogeler, Braaten, Slesak, & Falkowski, 2018). A different sensor type and a different acquisition time may have a large influence on the result of time series analysis. For this reason, relative radiometric normalization was used to eliminate the influence of different acquisition times, different phenological phases of vegetation, and the influence from the different spectral and radiometric characteristics of different sensors. Problems caused by the different times and locations of acquisition, the different positions of the Sun, and different radiometric and spectral differences can be reduced via normalization.

The PIF-Based Linear Regression method was selected for normalization on the basis of previous empirical testing that was carried out in several previous studies (Chen, Vierling, & Deering, 2005; Rahman, Hay, Couloigner, Hemachandran, & Bailin, 2015; Song, Woodcock, Seto, Lenney, & Macomber, 2001), and testing of the relative radiometric normalizations in the article by Lastovicka, Hladky, Stych, and Holman (2017). The PIF-Based Linear Regression method is a relatively standard proven

Table 2. Description of the sites of interest (source: NAPANT).

Locality	Treatment	Disturbance	Site name	Valley name	Coordinates (ETRS89)	
1	managed	Wind	Veľký Gápeľ	Zelenská Mlynná	48.9049668	19.6364943
2	managed	Wind	Trangoška I.	Bystrá	48.9246311	19.6134983
3	managed	Wind	Trangoška II.	Bystrá	48.9223156	19.6047867
4	unprocessed	Bark Beetle	Králičká	Zelenská Mlynná	48.9157142	19.6521710
5	unprocessed	Bark Beetle	Kosodrevina I.	Bystrá	48.9293947	19.5935642
6	unprocessed	Bark Beetle	Kološňa	Bystrá	48.9291619	19.6088744
7	semi-natural	No	Malý Gápeľ	Pošova Mlynná	48.9005580	19.6533417
8	semi-natural	No	Zadné Dereše	Bystrá	48.9272675	19.5836911
9	semi-natural	No	Kosodrevina II.	Bystrá	48.9310644	19.6011869

method, which has its origins in the 1990s, and is probably the most commonly used technique with MAD/IR-MAD. Many variations of PIF are used in algorithms for investigating time series (e.g. MAD/IR-MAD by Canty & Nielsen, 2008; Schroeder, Cohen, Song, Canty, & Yang, 2006; Syariz et al., 2019). The PIF-Based Linear Regression method is based on linear alignment using linear regression. In this method, a traditional linear regression is used in which the approximation of the known values is represented by the smallest square method.

The method consists of finding pseudo-invariant objects via the use of the invariant objects in two observed images (reference – master and compared – slave, where the PIF-Based Linear Regression method uses one reference image from the middle of the observation period and the others as slaves) that occur as clusters in a scatter plot (Chen et al., 2005; Mei, Bassani, Fontinovo, Salvatori, & Allegrini, 2016; Schroeder et al., 2006; Song et al., 2001; Yang & Lo, 2000). The invariant values of both images are searched and selected manually or automatically using an algorithm (Bao et al., 2012). The master image for normalization selected was from 19 July 2006 (Landsat 5), the center of the observation period (Table 1). The invariant areas required for this method were selected using the NDVI index and the semi-automatic selection method inspired by Bao et al. (2012) and Chen et al. (2005). Pixels with values higher than 0 and lower than 0.5 were selected from the master image as a mask for the potential invariant features. Subsequently, this mask was applied to all the slave images (all the spectral bands). The individual master and slave bands were then compared for the remaining potential invariant elements. Based on the calculation of values for the surface reflectance of unchanged land cover types (primarily urban areas, town squares, and roads) for the different types of sensors (e.g. Landsat 5 vs. Landsat 8), the range of the unchanging values was found. Based on this range, specific invariant pixels were selected to compare the master and slave images band by band. Thus, inverse regression by linear regression roots (via matching pairs of both images – band x of the reference image with band x of the slave image) was applied to the entire slave image (Chen et al., 2005).

For the data normalization and the time series visualization of the CDR Landsat data, custom semi-automatic applications were developed in the Matlab environment. The developed application was inspired by the TimeSync web application (Cohen, Yang, & Kennedy, 2010), which has limitations in accessing custom data as well as bulk data over the Internet. However, the application allows work with any type of satellite data to be carried out in an off-line mode. This application is transferable to a wide range of software and operating systems because of the relatively standardized Matlab encryption. The application itself consists of several algorithms for which two user interfaces have been created. The first user interface allows users to see the differences between the two spectral bands that are required for normalization purposes. The scatter graph and interdependence are displayed using a linear regression curve. The second user interface allows users to choose the destination and to create TS figures.

After the process of data standardization, selected vegetation indices were calculated in Envi 5.1, and time series charts created in our own Matlab app. The application then created time series charts for the specified locations. The calculations take the pixel values of the site or its surroundings (3x3 pixels) into account. In the case of this study, the closest neighborhood of the site was used, with 3×3 pixels. For a more detailed description of this application, see Lastovicka et al. (2017).

On the basis of previous studies such as Jin and Sader (2005) or Chen et al. (2005), it was decided that the visible, NIR, and SWIR bands would be used for the evaluation of the vegetation indices based on the use of spectral bands. Below is a list of the ratios used for vegetation indices:

(a) The NDVI (Normalized Difference Vegetation Index), which includes values from −1 to 1. In general, higher values of the NDVI reflect a higher amount of vegetation (Musilova, 2012; Wang et al., 2010).
(b) The Simple Ratio Index (SR, Equation 1), which demonstrates the inverse relationship between chlorophyll absorption in the red band and the increased reflection of the healthy vegetation in the near infrared band. The index assigns a value of 1 for bare soils and increases in value as the vegetation cover increases (Birth & McVey, 1968). It is determined using the relationship:

$$SR = \frac{NIR}{RED}$$

Equation 1. the Simple Ratio Index (SR)

(c) The NDMI (Normalized Difference Moisture Index, Equation 2) is an index for observing the water content in vegetation. This vegetation index is designed to look for disturbances in the landscape. The advantage of this index is the possibility of detecting the vegetation structures that have been only minimally disturbed (Jin & Sader, 2005).

$$NDMI = \frac{NIR - SWIR}{NIR + SWIR}$$

Equation 2. the Normalized Difference Moisture Index (NDMI)

(d) The FMI (Foliar Moisture Index, Equation 3) is designed to monitor the humidity ratios of vegetation (Wang et al., 2010). Its relationship is:

$$FMI = \frac{NIR}{RED \times SWIR}$$

Equation 3. the Foliar Moisture Index (FMI)

(e) The wNDII (wide-band Normalized Difference Infrared Index, Equation 4) is also used to determine the humidity of the vegetation. It is mainly used to estimate the moisture in a leaf per unit area (Musilova, 2012; Wang et al., 2010). It is determined by the relationship:

$$wNDII = \frac{2NIR - SWIR}{2NIR + SWIR}$$

Equation 4. the wide-band Normalized Difference Infrared Index (wNDII)

(f) The slightly modified NDVI index, which does not take negative values, is called the TVI (Transformed Vegetation Index, Equation 5, Rouse, Hass, Schell, & Deering, 1973). The significance of the second power in the relationship is to repair the Poisson distribution of the NDVI values to normal ones. The index is suitable for masking the influence of the soil, similar to SAVI. Its relationship index:

$$TVI = \sqrt{\frac{(NIR - RED)}{(NIR + RED)} + 0,5}$$

Equation 5. the Transformed Vegetation Index (TVI)

The TS graphs were created using the above-mentioned applications and represent the average values in the location observed (3 x 3 pixels) in the selected index for the entire observation period. The center of the site of interest was selected as the location from which observation was carried out. This method eliminated any discrepancies that could occur during the resampling of the images and eliminated any overlapping with areas outside the site of interest.

Results

The results are focused on describing and interpreting the value of the vegetation indices in the 9 different case studies where different types of development has occurred in the forest (localities 1–3 were influenced by a damage from wind, localities 4–6 were affected by a bark beetle invasion, and localities 7–9 were forest vegetation that was unaffected by any significant disturbance). The similarities and differences in the values for the studied indices are presented with respect to the evaluation of the particular disturbances. The results describe and interpret the values of the studied vegetation indices during the observed period and evaluate the suitability of these indices for the assessment of changes in the forest. The results should indicate the applicability of different vegetation indices or combinations of these for the detection of different types of disturbances.

Localities 1-3 (with wind disturbance)

A significant part of the Low Tatras National Park was damaged by the catastrophe caused by winds during storm Elizabeth, which took place on 19 November 2004, and the associated abiotic disturbances that occurred over the next few years. The first three sites to be explored represent the area which was most heavily damaged by this event, followed by the semi-natural regeneration of the vegetation after the calamity.

Elimination of the consequences of this catastrophe was managed economically only after accessibility to the locality became available through the construction of a forest road network after 2008. The damaged trunks were removed from the site, but approximately 10–30% of the mass of wood destroyed by the catastrophe was left in place. The restoration of the forest took place via both natural and forestry-controlled regeneration. In this case, the area was occupied primarily by berry species (*Vaccinium myrtillus, Rubus fruticosus, Rubus idaeus*), rowan (*Sorbus aucuparia*), and lichens. Young spruces were planted by the foresters to support the recovery of the forest.

The results of the development of the individual monitored indices are documented in Figures 2–4. The changes in the values for the monitored indices indicate that the 2004 gales significantly affected the state of the forest vegetation in all three localities. The indices strongly reflect this wind disaster, and a significant change is observed in all the values. An accurate assessment of the impact of a disturbance is difficult for the period immediately following the event because of the lack of suitable Landsat images from between 2001–2005. However, images from the subsequent years can be used to specify the disturbance, which is evident from the resulting curves. The sudden damage to the vegetation is reflected in the apparent decrease in the values of the observed vegetation indices. It can be seen from Figures 2–4 that the most significant changes (decreases) are apparent in the values of the vegetation indices NDVI, NDMI, and wNDII; the decline in the curve is minor in the FMI, SR, and TVI indices. According to the forest management plan and field observation, many of the tree

trunks (mostly spruce) were left at the site following the disaster, and after 2006 it was possible to observe both the natural and forestry-controlled regeneration of the vegetation. According to the in-situ data, the vegetation gradually began to cover the affected site, and the land gradually became dominated by shrubs. All of the indices reflected the sudden destruction of the forests with the subsequent death of the trees by a significant drop in values. Forest undergrowth is recorded in the NDVI, NDMI, and wNDII index trajectories with a gradual but noticeable increase in the values. A significant change in the NDMI values occurred in localities 2 and 3 (see Figures 3–4). Lower values were recorded in the SR index while the vegetation was restored, but no increase could be seen in the values of the FMI index as a respond to this regeneration. It is apparent that there is a very similar trend in all localities from the curves describing the different localities for the same type (wind disturbance). We note only minor differences in the values in the graphs. In the period before and after the calamity, only minor fluctuations can be seen in the figures, which could be primarily caused by changes in the phenological

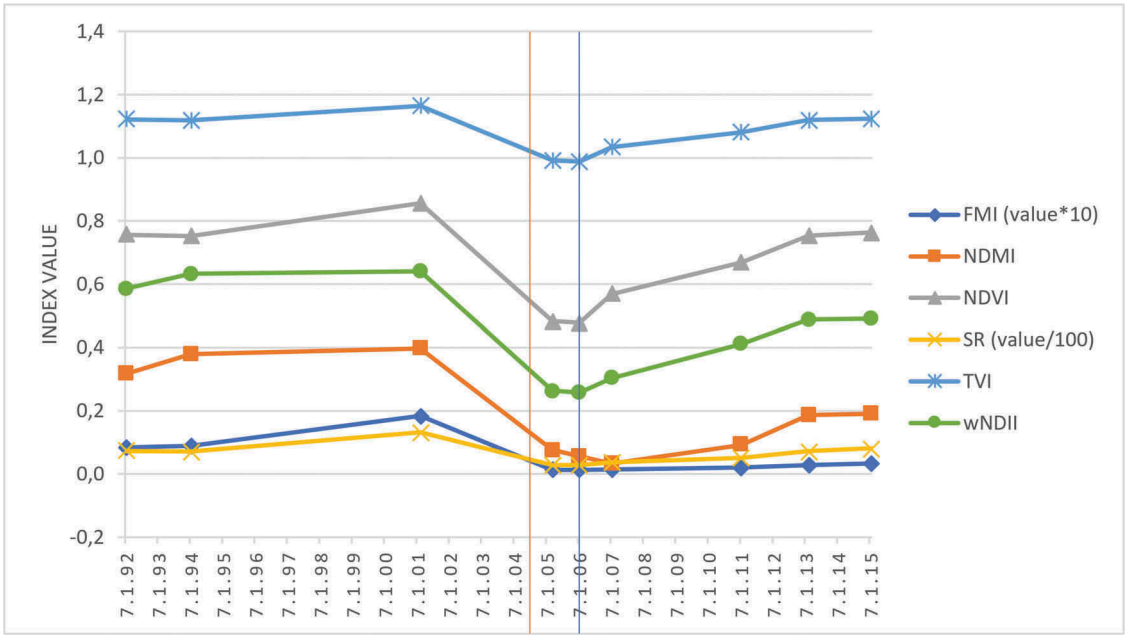

Figure 2. The development of the individual monitored indices for the locality 1 affected by wind disturbance (red vertical line is the time of wind disturbance and blue line is the start of recovery mode) (source: own creation).

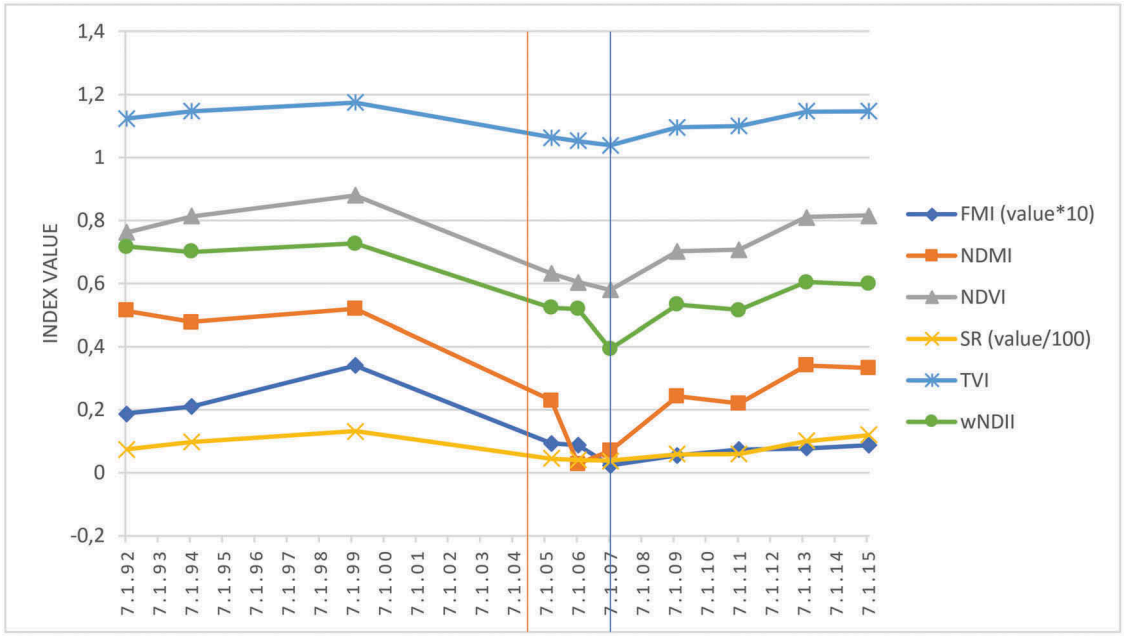

Figure 3. The development of the individual monitored indices for the locality 2 affected by wind disturbance (red vertical line is the time of wind disturbance and blue line is the start of recovery mode) (source: own creation).

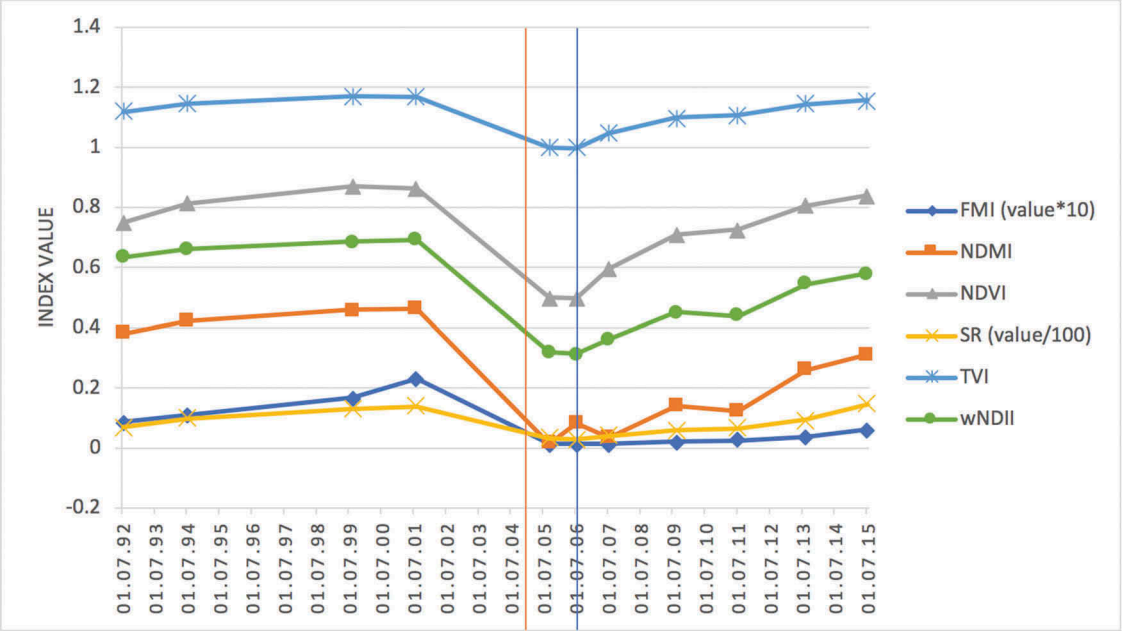

Figure 4. The development of the individual monitored indices for the locality 3 affected by wind disturbance (red vertical line is the time of wind disturbance and blue line is the start of recovery mode) (source: own creation).

phase or be due to external factors (e.g. weather conditions).

Localities 4-6 (with bark beetle disturbance)

The second category of observed sites (Figures 5–7) are the three sites that were affected by the strongly expanding, devastating bark beetle invasion that occurred following 2007. After the invasion, the forest vegetation was left dying and susceptible to other forms of biotic attack. Several obvious trends can be seen from the figures. At the beginning of the timeline (1992–1994), persistent or slightly increasing values can be observed in the vegetation indices, reflecting the natural development of forest vegetation. A role could also play different Landsat 4–8 data inputs for normalization, which achieved less accurate normalization results for Landsat 4 images. Consequently, most of the indices are characterized by a decline, not from 2007 when the bark calamity culminated, but from 2005, which was when the bark beetle catastrophe began, according to the forestry records. At this initiation phase, the vegetation indices wNDII, NDMI, and FMI declined, with the NDVI and TVI values oscillating between 2005 and 2007. At the peak period, all indices responded with a drop in value. A high similarity in these trends is seen in localities 4–6 in Figures 5–7. According to the forest records and in-situ data, the infectious wave spread over the entire forest after 2007. In the period 2007–2012, the observed sites are characterized by significant degradation and mass death of the spruce trees. All monitored indices responded with a change in values that continued until 2012, when a natural regeneration began, dominated by rowan (*Sorbus aucuparia*), which successively re-occupied the deforested areas. Many of the dried trunks of the still-standing dead spruce had fallen and become part of the vegetation and forest sub-growth by 2012. This was mainly reflected by the NDMI, wNDII, and NDVI indices, from which it is apparent that there was an increase in pioneer forest biomass that was gradually growing near the scattered dead spruce. The wNDII, NDMI, and NDVI indices generally show relevant fluctuations in value, from which both the initiation and the subsequent stages of the bark beetle invasion can be detected.

Localities 7-9 (without disturbance)

The final observations are for the investigation of localities where, unlike the two previous categories, there were no significant changes in the vegetation due to biotic and abiotic disturbances. It can be seen from Figures 8–10 that relatively small changes occurred in the observed area. However, some oscillations are visible in the values of all the indices. An insignificant fluctuation was recorded in the index of TVI. The oscillations in the indices of NDVI, FMI, are more visible, with the most obvious oscillations in the wNDII and NDMI indices. In terms of interpretation, it is necessary to bear in mind that changes in the values of indices may reflect events other than anthropogenic impact, such as weather conditions (precipitation or drought). Certain oscillations/discontinuities in the values during the first few years observed (at the beginning of the charts) could be caused by the result

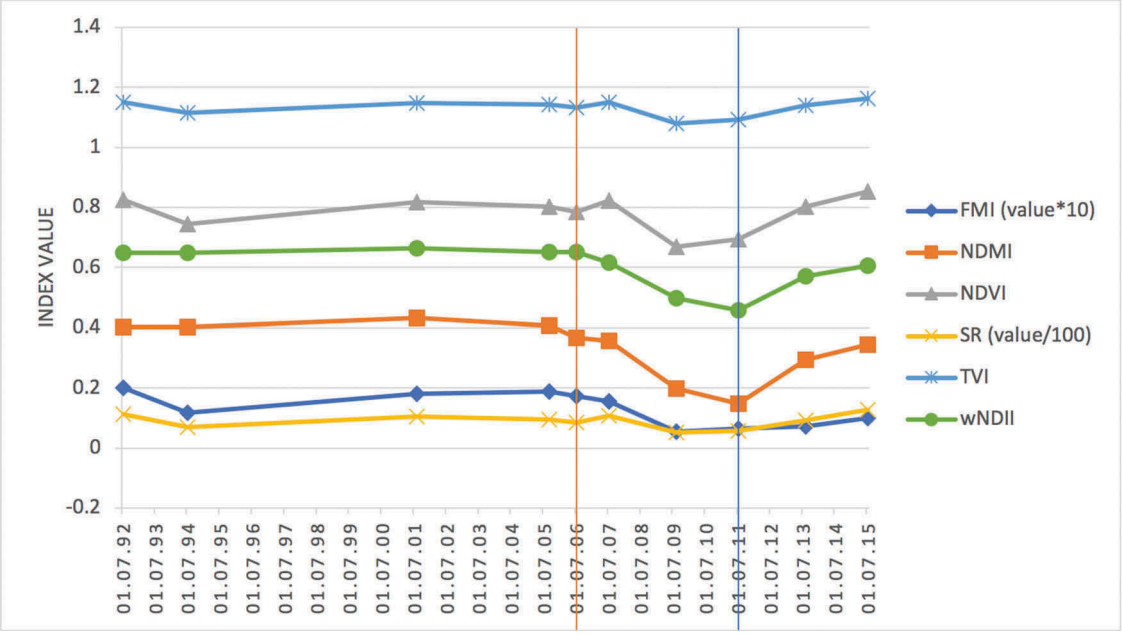

Figure 5. The development of the individual monitored indices for the locality 4 affected by bark beetle disturbance (red vertical line is the start of bark beetle disturbance and blue line is the start of recovery mode) (source: own creation).

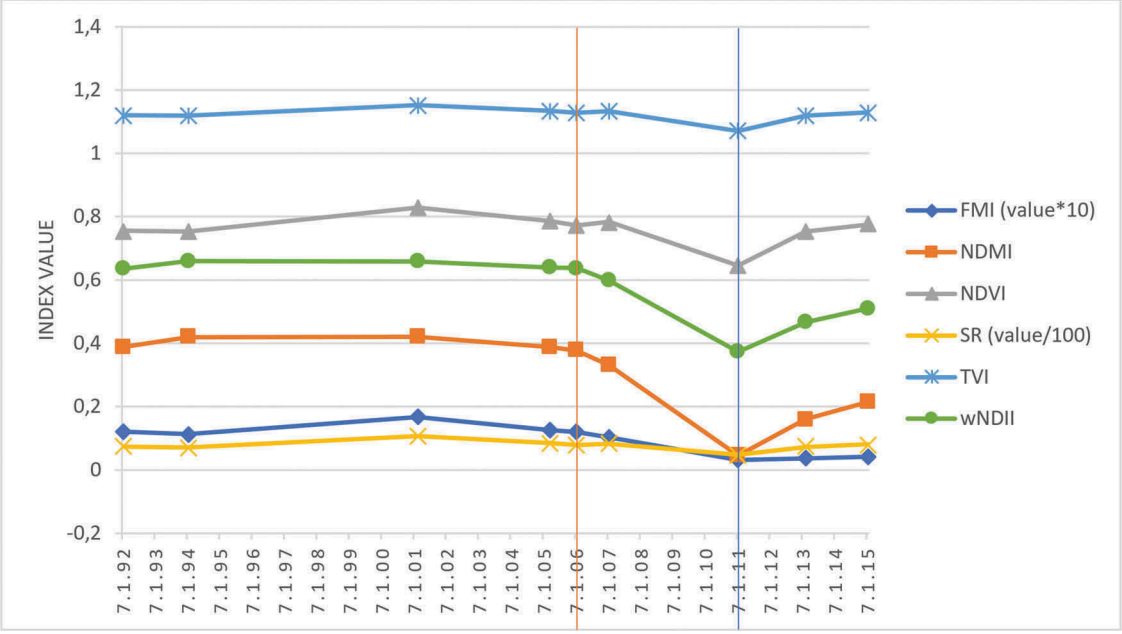

Figure 6. The development of the individual monitored indices for the locality 5 affected by bark beetle disturbance (red vertical line is the start of bark beetle disturbance and blue line is the start of recovery mode) (source: own creation).

of the lower accuracy in the normalization of Landsat 4.

Figure 8 (locality 7) shows an insignificant decrease in the first half of the observation period and lower values for the indices in the years 2005–2009. This could be related to previous deforestation that has occurred in the surroundings of this locality. The value of some of the peripheral pixels (the whole observed area was 3 × 3 pixels) could be influenced by this deforestation. In the second half of the period observed there is an obvious increase in the values reflecting the gradual afforestation in the surroundings. The remaining two localities (Figures 9 and 10) achieved higher average values and more stable development, because the wider surroundings of the sites observed were forested continuously during the observation period (see Attachment 9 and 10).

Discussion

It can be argued that if the effects of individual natural and anthropogenic factors are in equilibrium, the

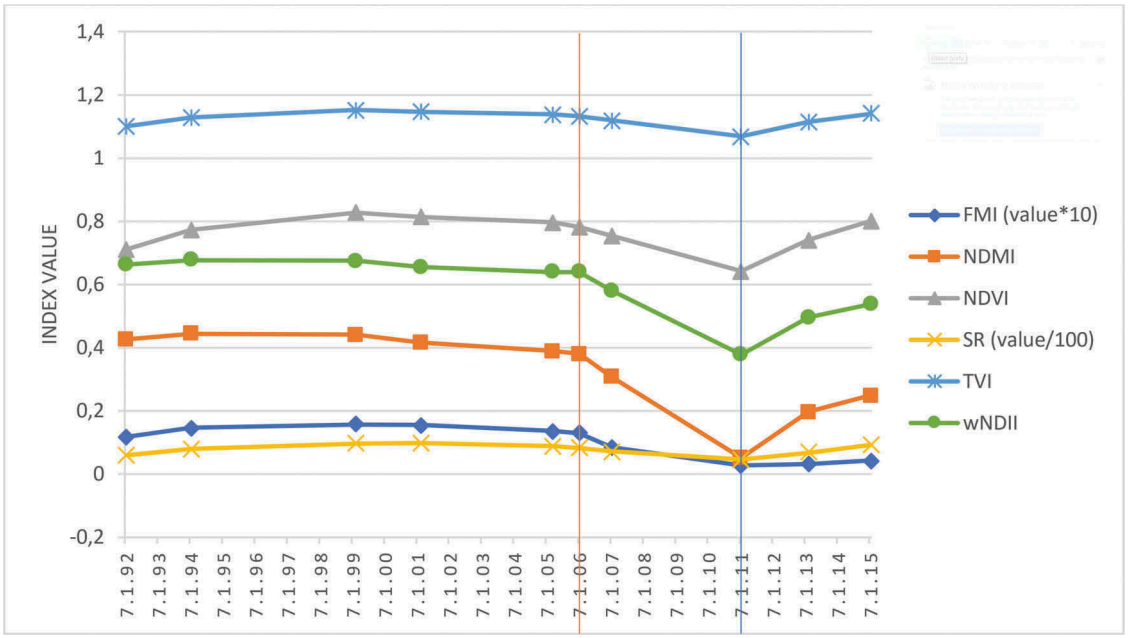

Figure 7. The development of the individual monitored indices for the locality 6 affected by bark beetle disturbance (red vertical line is the start of bark beetle disturbance and blue line is the start of recovery mode) (source: own creation).

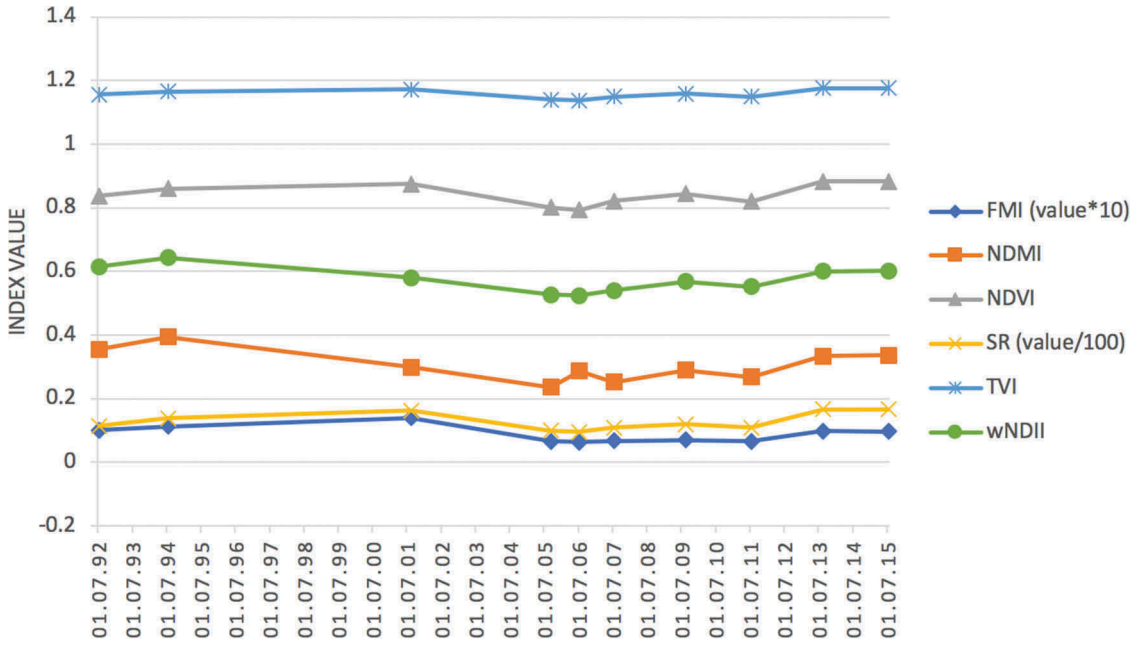

Figure 8. The development of the individual monitored indices for the locality 7 without disturbance (source: own creation).

ecosystem appears to be stable. When a certain factor prevails, including a natural factor (wind, bark beetles, etc.), there is a disruption or even an ecosystem breakdown in a manner that is usually associated with chain-linked concomitant disorders (Jakus & Stolina, 1997). It is well known that biotic pests can spread rapidly onto debilitated trees, typically after a previous abiotic catastrophe. Damage caused by severe winds may under certain conditions help these pests to reproduce. Decisions on the nature, extent, manner, and the timing of any measures to be implemented must be based on an objective and critical assessment of the autoregulatory capacity of the forest ecosystem and the environmental function that the forest has in the country concerned (Jakus & Stolina, 1997). One of the sites that was severely affected by both the windstorm and the subsequently crawling insect invasion was the upper border of the forest in the Low Tatras National Park (S-NAPANT Report, 2008).

The aim of this study was to determine the suitability of selected vegetation indices for capturing the phenomena of different types of biotic and abiotic disturbances in the selected localities of the Low Tatras National Park. Each type of disturbance, whether biotic or abiotic, has a specific manner by which it develops and different consequences for the state of the trees and changes in

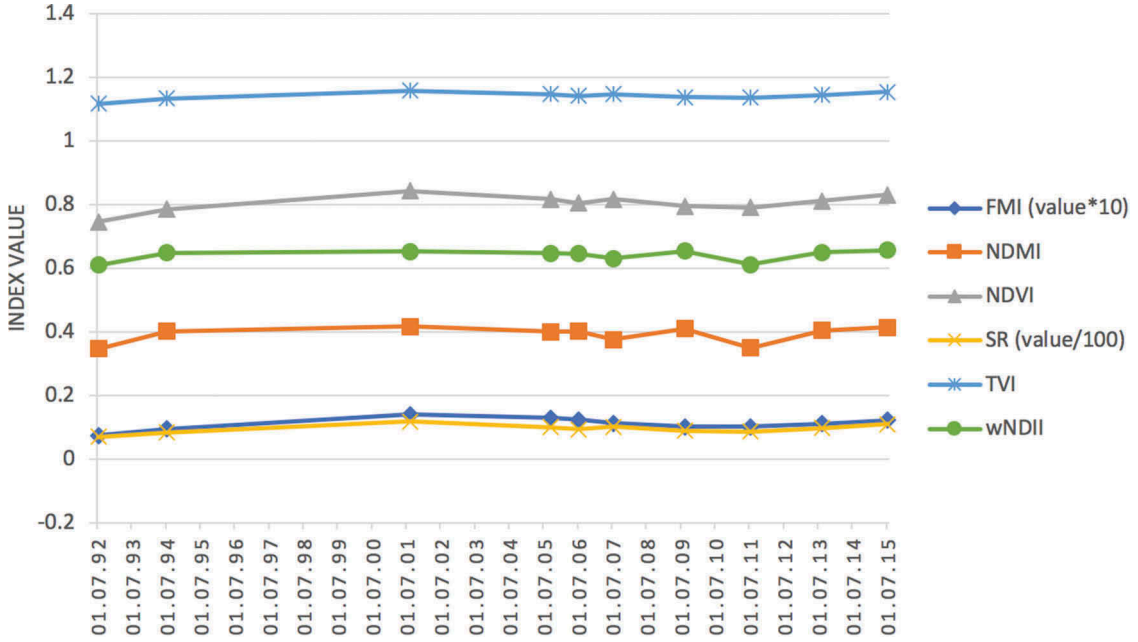

Figure 9. The development of the individual monitored indices for the locality 8 without disturbance (source: own creation).

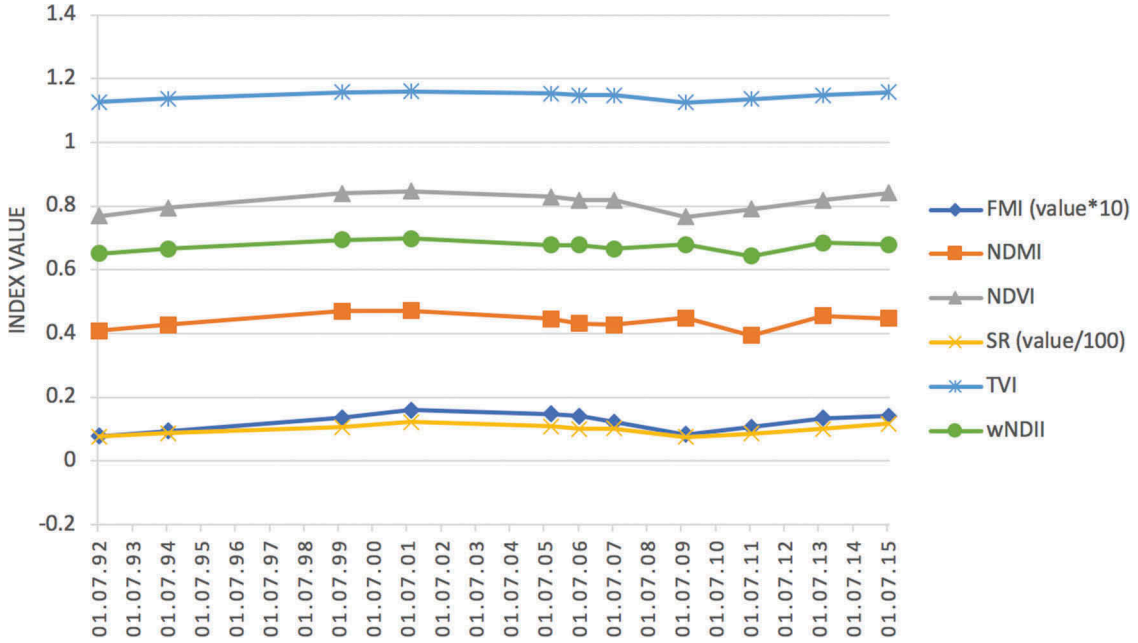

Figure 10. The development of the individual monitored indices for the locality 9 without disturbance (source: own creation).

the vegetation index value. A large part of the forest vegetation is usually devastated under strong wind disasters. The remaining forest vegetation is either damaged and dies later or becomes managed for forest renewal. This corresponds to a large decrease in the reflectance of near-infrared radiation (Cohen, Yang, Healey, Kennedy, & Gorelick, 2018). After intervention by the forestry services and the planting of new vegetation, the exposed floor allows the possibility of developing vegetation, and therefore a renewed increase is observed in the reflection of green light a relatively short time after the disturbance, especially in the infrared part of the spectrum.

When interpreting the changes that occur in the values of the vegetation index, the diversity of the forest during both attack and restoration must be considered, and the principles under which the indices are computed as well. When interpreting the values for the vegetation indices, knowledge of the nature of the vegetation, which affects many indices, also plays an important role. The degradation in the forest vegetation decreases the vitality and volume of the biomass. A decrease can be observed in the reflectivity of the NIR spectrum. Evidence of this in the TS vegetation indices is shown in Figures 2–4. The NDVI index

sharply declined with the windstorm in 2004, as the forest vegetation was severely damaged. Similarly, other vegetation indices responded accordingly.

However, the disaster caused by the presence of bark beetles is much more complicated, with effects that are more specific to the vegetation than in the case of wind turbulence. Initiation is predominantly due to a strong culmination of favorable conditions, when the primary deterioration in the health of the forest is mainly within a small area. The next generation of beetles gradually occupies the surroundings of the original site and three generations of beetle can be produced in one year, significantly degrading the resistance of the forest stand. In the case of bark beetles, high sensitivity can be seen in the vegetation indices wNDII and NDMI or FMI, all of which use SWIR bands. These vegetation indices were able to reflect the most relevant phases of the disturbance in the TS analysis. The reflectivity of the healthy forest vegetation in the SWIR is lower than in the NIR, and during the occurrence of the disturbance or damage the SWIR reflectivity is increased. It is clear from these results that this aspect played an important role, because many changes in the health status of the vegetation due to the disturbance indices using the SWIR bands responded sensitively (the NDMI or wNDII vegetation indices used in the calculation NIR and SWIR bands). An important result of this study is the discovery that the NDMI and wNDII vegetation indices can capture all stages of the bark beetle calamity (before, during, and after culmination) and are therefore suitable indicators for monitoring the health of the forest vegetation in such specific/environmentally complex processes as a bark beetle invasion with its causes and consequences. The NDVI or TVI vegetation indices based on the visible band and NIR ratios were able to record the peak culmination wave of the bark beetle invasion in the TS; however, this showed a different evolution in the initiation phase than the NDMI or wNDII indices.

At the sites which were not affected by any strongly disturbing influence in 1992–2015 according to the archive records, values of the studied vegetation indices (e.g. NDVI or TVI) did not change significantly. These types of vegetation indices are able to record the strongest disturbance effects on vegetation. Values of the indices wNDII and NDMI fluctuated more at the sites of the third group (Figures 8–10). From this point of view, it can be stated that indices using SWIR are sensitive to more environmental/external factors (Jensen, 2007). The values of the vegetation indices can be affected by many factors that were not included in this investigation, such as precipitation or soil moisture. For a more detailed interpretation of these changes, it would be necessary to include several other factors, such as meteorological factors, which is beyond the scope of this study.

Information obtained through satellite imagery can be applied to thematic areas in order to follow and evaluate aspects of forestry such as the changes in the woody structure of mountain forests, the increase and decrease in the representation of deciduous or coniferous trees and their subsistence in forests that were originally mixed, trends in the phytosociological changes to bushes and unprocessed fields, the occurrence of successive vegetation of woody plants on non-forested areas and uncultivated hollows, or the long-term monitoring of the climax forest status (Gloncak, 2009; Sitkova & Pavlenda, 2017). Landsat data allows us to remotely observe the Earth for the past 47 years (since 1972). It is therefore an important source of data for use with TS. An alternative of Landsat data can be seen in the data of Sentinel-2 produced by Copernicus. The advantage of the Sentinel-2 data is the higher spatial resolution (10 m for VIS/NIR and 20 m for NIR and SWIR bands) and the higher temporal resolution. Such a high temporal resolution (5 days) is guaranteed by the operation of two satellites (Sentinel-2A and Sentinel-2B) and by a wider swath width of 290 km (compared with the 185 km for Landsat 5 and the 120 km of SPOT). It has recently become possible to fuse data from different sensors. Several methods that are available have been tested, such as the harmonization algorithms LandTrendr (Kennedy, Yang, & Cohen, 2010; Yang et al., 2018) and LandsatLinkr (Vogeler et al., 2018). A cross-sensor compatibility has been tested with Landsat and Sentinel data by using BRDF normalization (Roy et al., 2016) as a result of the HLS (Harmonized Landsat and Sentinel) dataset (Claverie et al., 2018), which provides excellent temporal coverage in conjunction with high spatial resolution. From the point of view of time series analysis, cloud-based and big data technologies have become important with very useful tools. For example, Google Earth (Xie et al., 2019) and Sentinel-Hub (Sovdat, Kadunc, Batic, & Milcinski, 2019) allow the processing of large amounts of data in a very short time without needing to download the original data. These applications therefore represent prospective technologies in time series research using remote sensing data. In completing this article, we worked

closely with the administration of Low Tatras National Park. Based on the findings of this potential end-user of the data and the RS method, a broad offer and the prospective of a long-term observation mechanism for individual thematic issues will become accessible in the future. It is necessary to design and define this with regards to the distinctive and temporal possibilities of the available satellite imagery. The application level is also important from an economic point of view, wherein the affordability and availability of allowing end-users to access data from Landsat or Sentinel and methods of RS with greater emphasis and efficiency. As an example of the Low Tatras National Park, some possible satellite data applications can be identified that would be useful and usable for the practical side of the decision-making processes inherent to conservation, assessing the development and knowledge of the current state of the natural and socio-economic aspects of the landscape or the individual components of the environment.

An important finding gained in this study is the high relevance of forest management data and NAPANT field research records. The data contained in the forest management plans appears to be excellent as a source for the validation of the results of TS investigation and is potentially a highly suitable source of information for classifying the species composition of a forest. The forest management plans contain a wide range of useful information that is regularly updated. Data from the field surveys of NAPANT provided highly detailed data on the recovery of the forest ecosystems, especially with regards to the restoration of the herbaceous and woody undergrowth.

The issue of the monitoring and evaluation of the impact from disturbances can open up a wide-ranging discussion on the assessment of forest management practices, assessing the age, spatial, and species differentiation of a forest, and assessing the stability of a forest ecosystems (Vladovic, 2003). Significant attention should be paid to the occurrence of spruce stands, which is generally attributed to soil fatigue by the repeated cultivation of spruce, air pollution, and in particular the increased activity of sub-insects and fungal pathogens (Kunca & Zubrik, 2012). Possibly, and in the long term, it is necessary to monitor the changes in the state and development of the grass cover due to grazing (mowing, wandering livestock), ruderalization and its remnants from previous ages or the decline of traditional farming methods. Another important issue that affects forest ecosystems is the construction/expansion of the forest transport network and tourist areas (Polak & Saxa, 2005). Climate change is also expected to affect the forests, with the gradually rising temperature and changing temperature regimes. From this point of view, the long-term monitoring archive of the satellite data is a great advantage, as well as the exact location of the object/phenomenon monitored.

In conclusion, the use of satellite data to evaluate the consequences of differentiated approaches to conservation and forestry activities provides the opportunity to monitor and compare the state of vegetation and its response to the method of protection and management used in sites of a similar nature. Suggestions for a comparative study and potential cooperation with the Low Tatras National Park administration can be found in the National Park of Sumava in the Czech Republic or in the Bavarian Forest National Park in Germany (Hais et al., 2009a).

Conclusions

From our results, we can state that the Landsat time series and the calculated values of the vegetation indices appear to be highly useful methods for assessing the health status of forest vegetation. Freely available Landsat data is a very useful data source in this respect. It is also necessary to pay attention to the compatibility of data from various types of Landsat sensors. Although Landsat CDR data includes atmospheric and radiometric corrections, it is still useful to perform radiometric normalization. Because of this normalization, the effects of different times and places of acquisition, different positions of the Sun, and different radiometric and spectral differences can be reduced. The PIF-Based Linear Regression method (and other methods based on PIF, such as MAD/IR-MAD, see e.g. Syariz et al., 2019) appears to be a suitable normalization method for the normalization of images from different acquisition times, those influenced by various factors (e.g. inhomogeneity of the environment or volatility in the sensor measurements). In terms of the utilization of vegetation indices, this article focused on the evaluation of the most frequently used and recommended vegetation indices (FMI, NDMI, NDVI, wNDII, TVI, SR). The most accurate results were achieved using the NDMI index, which precisely reflected the changes in the forest cover that was caused by the disturbances.

This study should serve as an example for the application of remote sensing data when the impact of disturbances on forest vegetation is analyzed using vegetation indices. These results and methods should be useful and inspirational for the management of protected areas in order to determine the appropriate forest management practices under circumstances of forest disasters.

Attachment 1: Locality 1

Table 3. Description of the locality 1 (source: LGIS National Forest Center, GIS S-NAPANT).

	Locality 1 (Veľký Gápeľ/Zelenská Mlynná valley)	
Disturbance	Wind/managed	
Terrain parameters	Elevation: 1 305 m a.s.l. Slope: 65% Aspect: East	
Forest vegetation level (*group of forest types*)**, Corine Land Cover (2012) class**	Level 6 – spruce-beech fir; (*Fagetum abietino – piceosum*); CLC (2012) 324 Transitional woodland-shrub	
Forest (sub)category	O – protective forests (d- other forests with a predominant soil protection function)	
Described forest area (in year)	12,30 ha (1999)	8,10 ha (2009)
Forest age	145	5
Representation of tree species in % (described forest area-described year)		
Picea abies	50	15
Fagus sylvatica	35	-
Abies alba	15	-
Sorbus aucuparia	-	85

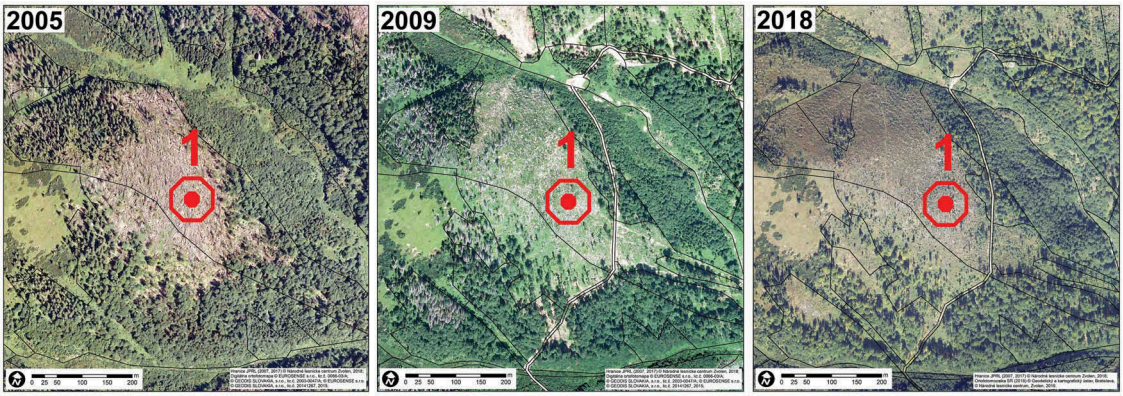

Figure 11. Aerial photographs of the locality 1 from years 2005, 2009 and 2018 (source: NAPANT, own creation).

Figure 12. Photo of the locality 1 (source: own creation).

Attachment 2: Locality 2

Table 4. Description of the locality 2 (source: LGIS National Forest Center, GIS S-NAPANT).

	Locality 2 (Trangoška l./Bystrá valley)	
Disturbance	Wind/managed	
Terrain parameters	Elevation: 1 180 m a.s.l. Slope: 65% Aspect: North	
Forest vegetation level (*group of forest types*), Corine Land Cover (2012) class	Level 6 – spruce-beech fir; (*Fagetum abietino – piceosum*); CLC (2012) 312 Coniferous forest	
Forest (sub)category	O – protective forests (d- other forests with a predominant soil protection function)	
Described forest area (in year)	14,43 ha (1999)	2,60 ha (2009)
Forest age	55	5
Representation of tree species in % (described forest area-described year)		
Picea abies	90	90
Abies alba	5	-
Sorbus aucuparia	-	10
Pinus cembra	5	-

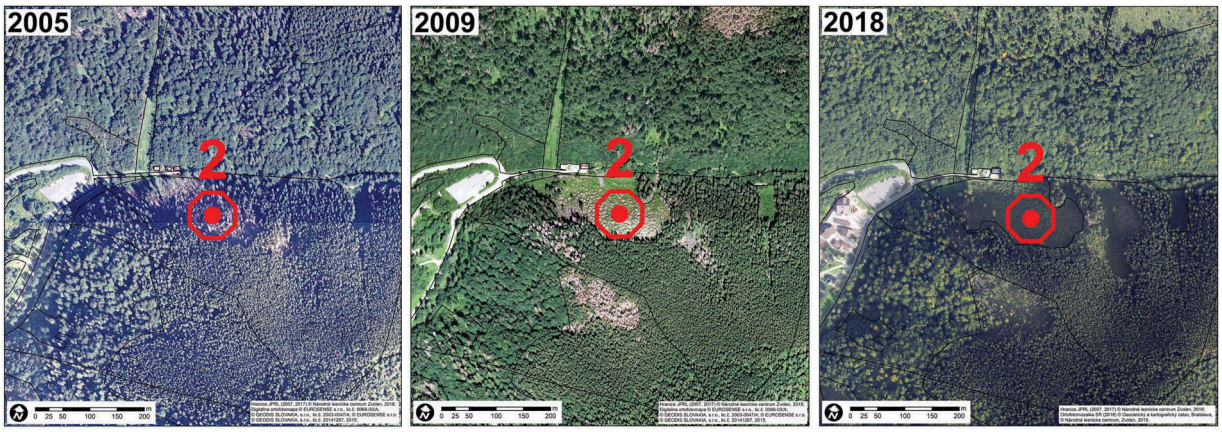

Figure 13. Aerial photographs of the locality 2 from years 2005, 2009 and 2018 (source: NAPANT, own creation).

Figure 14. Photo of the locality 2 (source: own creation).

Attachment 3: Locality 3

Table 5. Description of the locality 3 (source: LGIS National Forest Center, GIS S-NAPANT).

	Locality 3 (Trangoška II./Bystrá valley)	
Disturbance	Wind/managed	
Terrain parameters	Elevation: 1 125 m a.s.l. Slope: 27% Aspect: South	
Forest vegetation level (*group of forest types*), Corine Land Cover (2012) class	Level 6 – spruce-beech fir; (*Fagetum abietino – piceosum*); CLC (2012) 313 Mixed forest	
Forest (sub)category	O – protective forests (d- other forests with a predominant soil protection function)	
Described forest area (in year)	5,75 ha (1999)	2,79 ha (2009)
Forest age	60	0
Representation of tree species in % (described forest area-described year)		
Picea abies	85	-
Abies alba	10	-
Fagus sylvatica	5	-

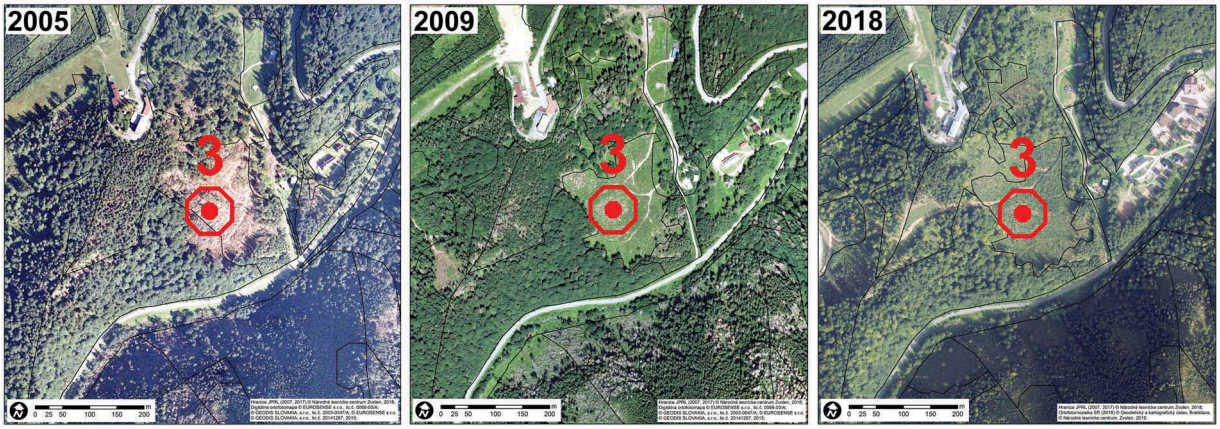

Figure 15. Aerial photographs of the locality 3 from years 2005, 2009 and 2018 (source: NAPANT, own creation).

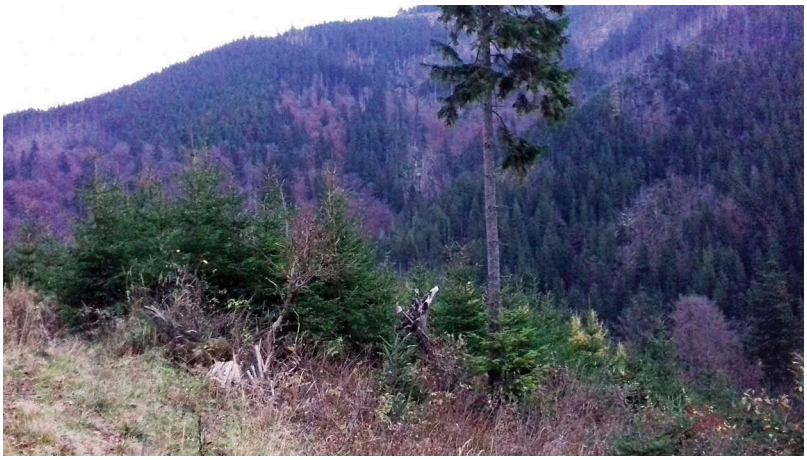

Figure 16. Photo of the locality 3 (source: own creation).

Attachment 4: Locality 4

Table 6. Description of the locality 4 (source: LGIS National Forest Center, GIS S-NAPANT).

	Locality 4 (Králička/Zelenská Mlynná valley)	
Disturbance	Bark Beetle/unprocessed	
Terrain parameters	Elevation: 1 500 m a.s.l. Slope: 57% Aspect: West	
Forest vegetation level (*group of forest types*), Corine Land Cover (2012) class	Level 7 – spruce; (*Sorbeto – Piceetum*); CLC (2012) 322 Moors and heathland	
Forest (sub)category	O – protective forests (b- forests below the upper limit of tree vegetation)	
Described forest area (in year)	13,10 ha (1999)	11,40 ha (2009)
Forest age	170	5
Representation of tree species in % (described forest area-described year)		
Picea abies	75	30
Abies alba	-	10
Fagus sylvatica	25	10
Sorbus aucuparia	-	50

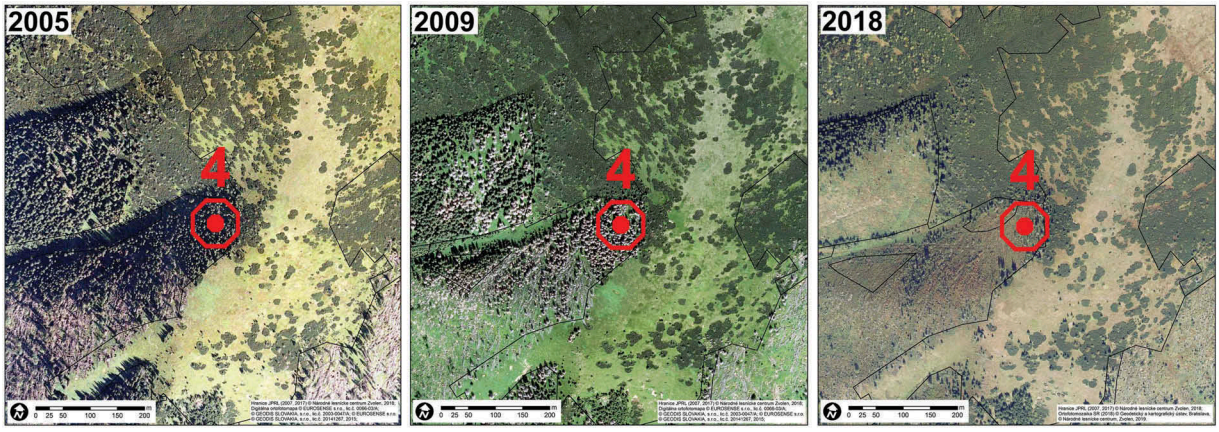

Figure 17. Aerial photographs of the locality 4 from years 2005, 2009 and 2018 (source: NAPANT, own creation).

Figure 18. Photo of the locality 4 (source: own creation).

Attachment 5: Locality 5

Table 7. Description of the locality 5 (source: LGIS National Forest Center, GIS S-NAPANT).

	Locality 5 (Kosodrevina l./Bystrá valley)	
Disturbance	Bark Beetle/unprocessed	
Terrain parameters	Elevation: 1 365 m a.s.l. Slope: 51% Aspect: South	
Forest vegetation level (*group of forest types*), Corine Land Cover (2012) class	Level 7 – spruce; (*Sorbeto – Piceetum*); CLC (2012) 312 Coniferous forest	
Forest (sub)category	O – protective forests (b- forests below the upper limit of tree vegetation)	
Described forest area (in year)	15,80 ha (1999)	15,80 ha (2009)
Forest age	160	170
Representation of tree species in % (described forest area-described year)		
Picea abies	95	95
Pinus mugo	5	5

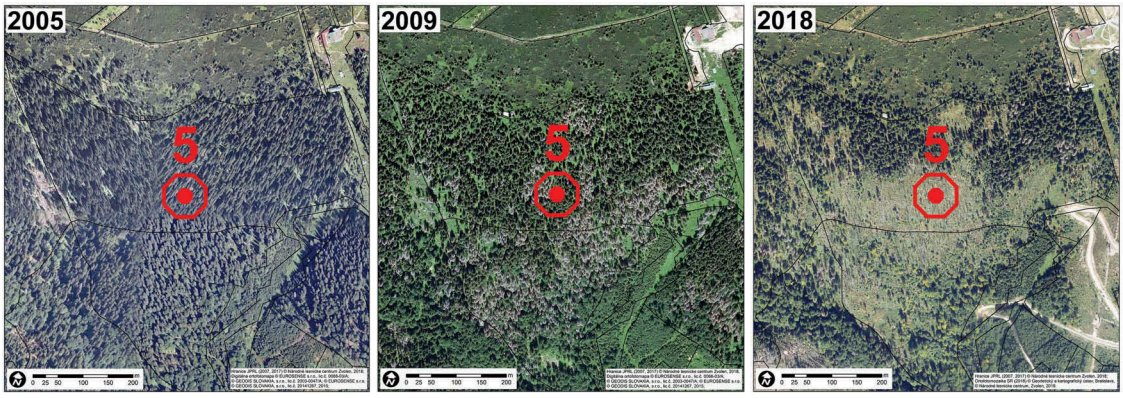

Figure 19. Aerial photographs of the locality 5 from years 2005, 2009 and 2018 (source: NAPANT, own creation).

Figure 20. Photo of the locality 5 (source: own creation).

Attachment 6: Locality 6

Table 8. Description of the locality 6 (source: LGIS National Forest Center, GIS S-NAPANT).

	Locality 6 (Kološňa/Bystrá valley)	
Disturbance	Bark Beetle/unprocessed	
Terrain parameters	Elevation: 1 360 m a.s.l. Slope: 48% Aspect: Southwest	
Forest vegetation level (*group of forest types*)**, Corine Land Cover (2012) class**	Level 7 – spruce; (*Sorbeto – Piceetum*); CLC (2012) 312 Coniferous forest	
Forest (sub)category	O – protective forests (b- forests below the upper limit of tree vegetation)	
Described forest area (in year)	12,10 ha (1999)	12,10 ha (2009)
Forest age	145	5
Representation of tree species in % (described forest area-described year)		
Picea abies	100	10
Fagus sylvatica	-	60
Sorbus aucuparia	-	30

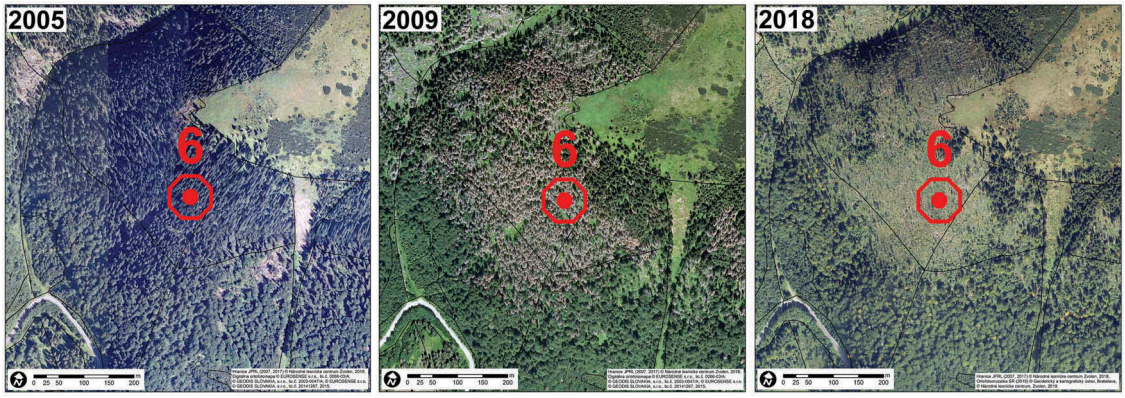

Figure 21. Aerial photographs of the locality 6 from years 2005, 2009 and 2018 (source: NAPANT, own creation).

Figure 22. Photo of the locality 6 (source: own creation).

Attachment 7: Locality 7

Table 9. Description of the locality 7 (source: LGIS National Forest Center, GIS S-NAPANT).

	Locality 7 (Malý Gápeľ/Pošova Mlynná valley)	
Disturbance	Low/No/semi-natural	
Terrain parameters	Elevation: 1 190 m a.s.l. Slope: 55% Aspect: Southwest	
Forest vegetation level (*group of forest types*), Corine Land Cover (2012) class	Level 6 – spruce-beech fir; (Fageto – Abietum, *Abieto-Fagetum*); CLC (2012) 313 Mixed forest	
Forest (sub)category	O – protective forests (d- other forests with a predominant soil protection function)	
Described forest area (in year)	5,12 ha (1999)	4,68 ha (2009)
Forest age	160	170
Representation of tree species in % (described forest area-described year)		
Picea abies	25	5
Abies alba	25	20
Fagus sylvatica	50	70
Acer pseudoplatanus		5

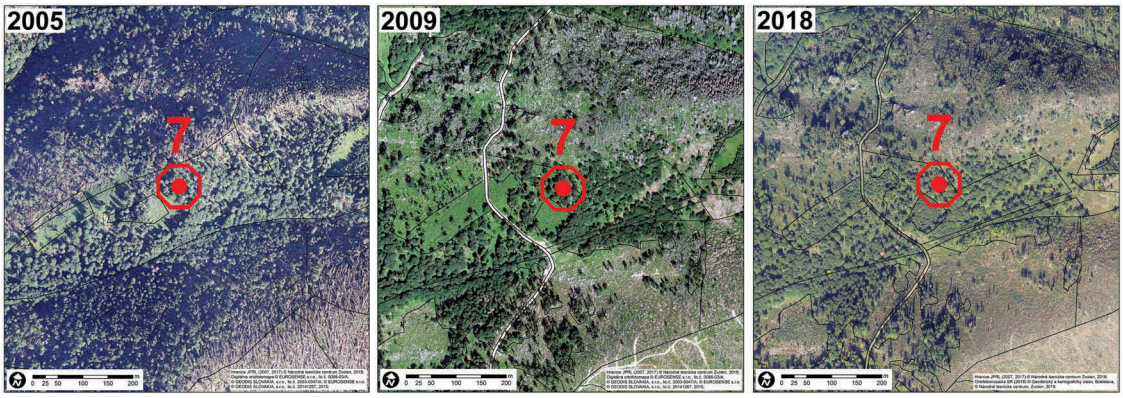

Figure 23. Aerial photographs of the locality 7 from years 2005, 2009 and 2018 (source: NAPANT, own creation).

Figure 24. Photo of the locality 7 (source: own creation).

Attachment 8: Locality 8

Table 10. Description of the locality 8 (source: LGIS National Forest Center, GIS S-NAPANT).

	Locality 8 (Zadné Dereše/Bystrá valley)	
Disturbance	Low/No/semi-natural	
Terrain parameters	Elevation: 1 430 m a.s.l. Slope: 39% Aspect: South	
Forest vegetation level (*group of forest types*), Corine Land Cover (2012) class	Level 7 – spruce; (*Sorbeto – Piceetum*); CLC (2012) 322 Moors and heathland	
Forest (sub)category	O – protective forests (b- forests below the upper limit of tree vegetation)	
Described forest area (in year)	11,60 ha (1999)	9,31 ha (2009)
Forest age	140	150
Representation of tree species in % (described forest area-described year)		
Picea abies	100	100

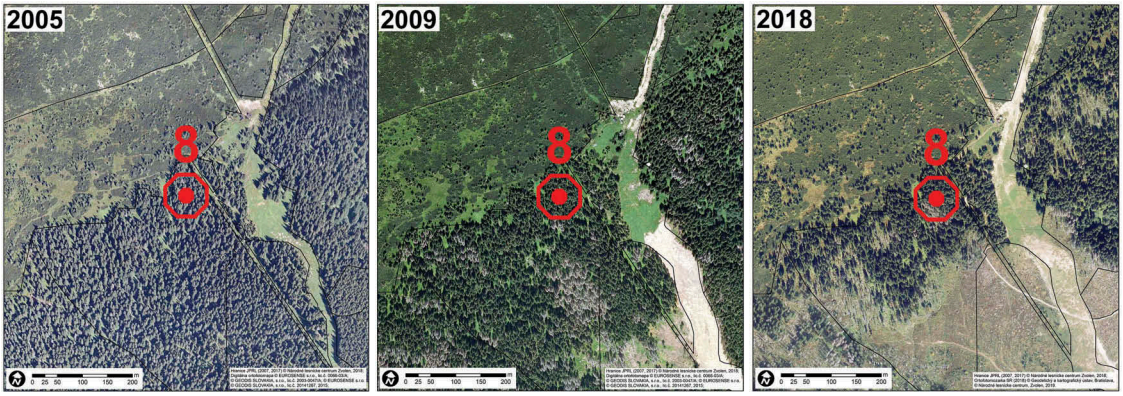

Figure 25. Aerial photographs of the locality 8 from years 2005, 2009 and 2018 (source: NAPANT, own creation).

Figure 26. Photo of the locality 8 (source: own creation).

Attachment 9: Locality 9

Table 11. Description of the locality 9 (source: LGIS National Forest Center, GIS S-NAPANT).

	Locality 9 (Kosodrevina II./Bystrá valley)	
Disturbance	Low/No/semi-natural	
Terrain parameters	Elevation: 1 405 m a.s.l. Slope: 54% Aspect: Southeast	
Forest vegetation level (*group of forest types*), Corine Land Cover (2012) class	Level 7 – spruce; (*Sorbeto – Piceetum*); CLC (2012) 312 Coniferous forest	
Forest (sub)category	O – protective forests (b- forests below the upper limit of tree vegetation)	
Described forest area (in year)	3,50 ha (1999)	3,10 ha (2009)
Forest age	140	150
Representation of tree species in % (described forest area-described year)		
Picea abies	90	90
Pinus mugo	10	10

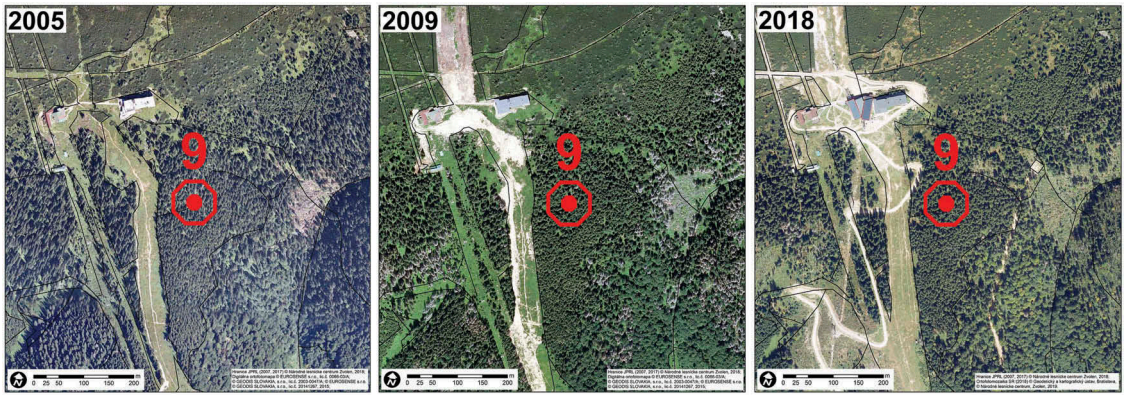

Figure 27. Aerial photographs of the locality 9 from years 2005, 2009 and 2018 (source: NAPANT, own creation).

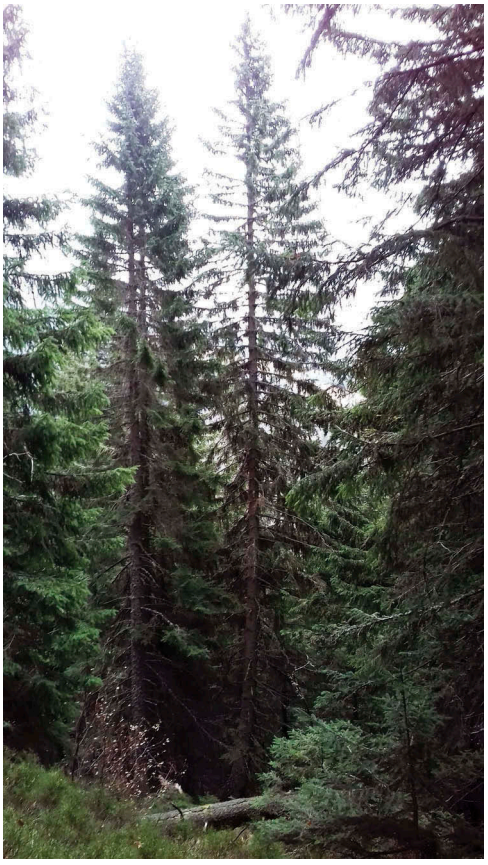

Figure 28. Photo of the locality 9 (source: own creation).

Acknowledgments

This work was supported by the GA UK (Charles University Grant Agency), Charles Univ, Fac Sci [GA UK Lastovicka 512217 (2017 - 2019)]; the European Union's Caroline Herschel Framework Partnership Agreement on Copernicus User Uptake under grant agreement No FPA 275/G/GRO/COPE/17/10042, project FPCUP (Framework Partnership Agreement on Copernicus User Uptake), Action 2019-2-49 "Developing supports for monitoring and reporting of GHG emissions and removals from land use, land use change and forestry (219/SI2.818795/07 (CLIMA)) and Charles University, Prague [Research Centre program UNCE/HUM/018].

Author Contributions

All authors contributed in a substantial way to the manuscript. Radovan Hladky and Josef Lastovicka designed and performed the research and wrote the manuscript. The authors collectively prepared the maps, figures, and tables. Premysl Stych is the senior author. He designed the research, contributed to writing the text, supervised the study, and reviewed the manuscript. Lukas Holman contributed to writing the text. All authors read and approved the submitted manuscript.

Conflict of Interest

The authors declare no conflict of interest

Disclosure statement

No potential conflict of interest was reported by the authors.

Funding

This work was supported by the GA UK (Charles University Grant Agency), Charles Univ, Fac Sci [GA UK Lastovicka 512217 (2017 - 2019)]; the European Union's Caroline Herschel Framework Partnership Agreement on Copernicus User Uptake under grant agreement No FPA 275/G/GRO/COPE/17/10042, project FPCUP (Framework Partnership Agreement on Copernicus User Uptake), Action 2019-2-49 "Developing supports for monitoring and reporting of GHG emissions and removals from land use, land use change and forestry (219/SI2.818795/07 (CLIMA)) and Charles University, Prague [Research Centre program UNCE/HUM/018].

ORCID

Premysl Stych http://orcid.org/0000-0002-0307-9688

References

Albrechtova, J., & Rock Barrett, N. (2003). Dalkovy pruzkum krusnohorskych lesu. *Vesmir, 82(322)*. Retrieved from https://vesmir.cz/cz/casopis/archiv-casopisu/2003/cislo-6/dalkovy-pruzkum-krusnohorskych-lesu.html

Bao, N., Lechner, A.M., Fletcher, A., Mulligan, D., Mellor, A., & Bai, Z. (2012). Comparison of relative radiometric normalization methods using pseudo-invariant features for change detection studies in rural and urban landscapes. *Journal of Applied Remote Sensing*, *6*. doi:10.1117/1.JRS.6.063578

Baumann, P.R. (2011, November 14–17). Landsat time series application: The Columbia Glacier, Canada – 1985 to 2010. In *Pecora 18-forty years of earth observation … understanding a changing world*. Herndon, Virginia. Retrieved from http://www.asprs.org/pecora18/proceedings/Baumann.pdf

Birth, G.S., & McVey, G.R. (1968). Measuring the color of growing turf with a reflectance spectrophotometer. *Agronomy Journal*, *60*, 640–643. doi:10.2134/agronj1968.00021962006000060016x

Bucha, T. (2014). *Satelity v sluzbach lesa* (pp. 202). Zvolen: Narodne lesnicke centrum. ISBN 978-80-89607-25-9.

Bucha, T., & Koreň, M. (2017). Phenology of the beech forests in the Western Carpathians from MODIS for 2000–2015. *iForest - Biogeosciences and Forestry*, *10*. doi:10.3832/IFOR2062-010

Butsic, V., Munteanu, C., Griffiths, P., Knorn, J., Radeloff, V. C., Lieskovsky, J., … Kuemmerle, T. (2017). The effect of protected areas on forest disturbance in the Carpathian Mountains 1985–2010. *Conservation Biology*, *31*(3), 570–580. doi:10.1111/cobi.12835

Campbell, P.K.E., Rock, B.N., Martin, M.E., Neefus, C.D., Irons, J.R., Middleton, E.M., & Albrechtova, J. (2004). Detection of initial damage in Norway spruce canopies using hyperspectral airborne data. *International Journal of Remote Sensing*, *25*(24), 5557–5584. doi:10.1080/01431160410001726058

Canty, M.J., & Nielsen, A.A. (2008). Automatic radiometric normalization of multitemporal satellite imagery with the iteratively re-weighted MAD transformation. *Remote Sensing of Environment*, *112*, 1025–1036. doi:10.1016/j.rse.2007.07.013

Chen, X., Vierling, L., & Deering, D. (2005). A simple and effective radiometric correction method to improve landscape change detection across sensors and across time. *Remote Sensing of Environment*, *98*(1), 63–79. doi:10.1016/j.rse.2005.05.021

Claverie, M., Ju, J., Masek, J.G., Dungan, J.L., Vermote, E.F., Roger, J.C., … Justice, C. (2018). The Harmonized Landsat and Sentinel-2 surface reflectance data set. *Remote Sensing of Environment*, *219*, 145–161. doi:10.1016/j.rse.2018.09.002

Cohen, W.B., Yang, Z., Healey, S.P., Kennedy, R.E., & Gorelick, N. (2018). A LandTrendr multispectral ensemble for forest disturbance detection. *Remote Sensing of Environment*, *205*(July 2017), 131–140. doi:10.1016/j.rse.2017.11.015

Cohen, W.B., Yang, Z., & Kennedy, R. (2010). Detecting trends in forest disturbance and recovery using yearly Landsat time series: 2. TimeSync - Tools for calibration and validation. *Remote Sensing of Environment*, *114*(12), 2911–2924. doi:10.1016/j.rse.2010.07.010

Entcheva, P., Rock, B.N., Martin, M., Albrechtova, J., Solcova, B., Tierney, M., & Irons, J. (1999, June 21–2). Remote sensing assessment of forest stress *in the* Western Bohemian Mountains of Central Europe – applications of ground and airborne spectrometry (GER2600 and ASAS). In *Fourth International Airborne Remote Sensing Conference and Exhibition/21 Canadian Symposium on*

Remote Sensing, Section H, Forestry; Ottawa, Canada, 128-143. doi:10.4315/0362-028x-62.2.128

Forkel, M., Carvalhais, N., Verbesselt, J., Mahecha, M.D., Neigh, C., & Reichstein, M. (2013). Trend change detection in NDVI time series: Effects of inter-annual variability and methodology. *Remote Sensing*, *5*(5), 2113–2144. doi:10.3390/rs5052113

Gloncak, P. (2009). *Dynamika vegetacie prirodnych horskych smrecin* (Dissertation thesis). Technicka univerzita vo Zvolene: depon in katedra fytologie.

Griffiths, P., Kuemmerle, T., Baumann, M., Radeloff, V. C., Abrudan, I.V., Lieskovsky, J., … Hostert, P. (2014). Forest disturbances, forest recovery, and changes in forest types across the Carpathian ecoregion from 1985 to 2010 based on landsat image composites. *Remote Sensing of Environment*, *151*, 72–88. doi:10.1016/j.rse.2013.04.022

Griffiths, P., Kuemmerle, T., Kennedy, R.E., Abrudan, I. V., Knorn, J., & Hostert, P. (2012). Using annual time-series of Landsat images to assess the effects of forest restitution in post-socialist Romania. *Remote Sensing of Environment*, *118*, 199–214. doi:10.1016/j.rse.2011.11.006

Hais, M., Jonasova, M., Langhammer, J., & Kucera, T. (2009a). Comparison of two types of forest disturbance using multitemporal Landsat TM/ETM+ imagery and field vegetation data. *Remote Sensing of Environment*, *113*(4), 835–845. doi:10.1016/j.rse.2008.12.012

Hais, M., & Kucera, T. (2009b). The influence of topography on the forest surface temperature retrieved from Landsat TM, ETM + and ASTER thermal channels. *ISPRS Journal of Photogrammetry and Remote Sensing*, *64*(6), 585–591. doi:10.1016/j.isprsjprs.2009.04.003

Hais, M., Wild, J., Berec, L., Bruna, J., Kennedy, R., Braaten, J., & Broz, Z. (2016). Landsat imagery spectral trajectories-important variables for spatially predicting the risks of bark beetle disturbance. *Remote Sensing*, *8* (8), 687. doi:10.3390/rs8080687

Hajek, F., & Svoboda, M. (2007). Vyhodnoceni odumirani horskeho smrkoveho lesa na Trojmezne (NP Sumava) metodou automatizovane klasifikace leteckych snimku Assessment of bark beetle damage in the Trojmezna old-growth. *Silva Gabreta*, *13*(1), 69–81.

Hansen, M.C., Stehman, S.V., & Potapov, P.V. (2010). Quantification of global gross forest cover loss. *Proceedings of the National Academy of Sciences of the United States of America*, *107*(19), 8650–8655. doi:10.1073/pnas.0912668107

Havasova, M., Bucha, T., Ferencik, J., & Jakus, R. (2015). Applicability of a vegetation indices-based method to map bark beetle outbreaks in the High Tatra Mountains. *Annals of Forest Research*, *58*(2), 295–310. doi:10.15287/afr.2015.388

Hlasny, T., Barka, I., Sitkova, Z., Bucha, T., Konopka, M., & Lukac, M. (2015). MODIS-based vegetation index has sufficient sensitivity to indicate stand-level intra-seasonal climatic stress in oak and beech forests. *Annals of Forest Science*, *72*(1), 109–125. doi:10.1007/s13595-014-0404-2

Hlasny, T., & Sitkova, Z. (2010). *Spruce forest decline in the Beskydy*. Zvolen: National Forest Centre – Forest Research Institute.

Jakobsen, H.H., Carstensen, J., Harrison, P.J., & Zingone, A. (2015). Estimating time series phytoplankton carbon biomass: Inter-lab comparison of species identification and comparison of volume-to-carbon scaling ratios. *Estuarine, Coastal and Shelf Science*, *162*, 143–150. doi:10.1016/j.ecss.2015.05.006

Jakus, R., & Stolina, M. (1997). Starostlivost o ekosystemy. In *Narodne parky, Sprava narodnych parkov SR, Tatranska Lomnica, 4/1997, 20-23.* ISSN 1335-23OX

Jensen, J.R. (2007). *Remote sensing of the environment: An earth resource perspective* (2nd ed.). Upper Saddle River: Pearson Prentice Hall.

Jin, S., & Sader, S.A. (2005). Comparison of time series tasseled cap wetness and the normalized difference moisture index in detecting forest disturbances. *Remote Sensing of Environment*, *94*(3), 364–372. doi:10.1016/j.rse.2004.10.012

Kennedy, R.E., Yang, Z., & Cohen, W.B. (2010). Detecting trends in forest disturbance and recovery using yearly Landsat time series: 1. LandTrendr - Temporal segmentation algorithms. *Remote Sensing of Environment*, *114*, 2897–2910. doi:10.1016/j.rse.2010.07.008

Kern, A., Marjanovic, H., Dobor, L., Anic, M., Hlasny, T., & Barcza, Z. (2017). Identification of years with extreme vegetation state in Central Europe based on remote sensing and meteorological data. *South-East European Forestry*, *8*(1), 1–20. doi:10.15177/seefor.17-05

Kozak, J. (2010). *Forest cover changes and their drivers in the polish carpathian mountains since 1800 BT - reforesting landscapes: linking pattern and process*. In H. Nagendra & J. Southworth (Eds.), (pp. 253–273). Dordrecht: Springer Netherlands. doi:10.1007/978-1-4020-9656-3_11

Kozak, J., Estreguil, C., & Troll, M. (2007). Forest cover changes in the northern Carpathians in the 20th century: A slow transition. *Journal of Land Use Science*, *2*(2), 127–146. doi:10.1080/17474230701218244

Kuemmerle, T., Hostert, P., Radeloff, V., Perzanowski, K., & Kruhlov, I. (2007). Post-socialist forest disturbance in the Carpathian border region of Poland, Slovakia, and Ukraine. *Ecological Applications: a Publication of the Ecological Society of America*, *17*, 1279–1295. doi:10.1890/06-1661.1

Kunca, A., Galko, J., & Zubrik, M. (2014). Vyznamne kalamity v lesoch Slovenska za poslednych 50 rokov. In A. Kunca (Ed.), *Aktualne problemy v ochrane lesa 2014, Zbornik referatov z 23. medzinarodnej konferencie konanej 23.-24.4.2014 v Kongresovom centre Kupelov Novy Smokovec, a.s* (pp. 25–31). Zvolen: Narodne lesnicke centrum.

Kunca, A., & Zubrik, M. (2012). *Problemy ochrany lesa na Slovensku*. Zvolen: Narodne lesnicke centrum - Lesnicky vyskumny ustav.

Kupkova, L., Cervena, L., Sucha, R., Jakesova, L., Zagajewski, B., Brezina, S., & Albrechtova, J. (2017). Classification of tundra vegetation in the Krkonose Mts. National park using APEX, AISA dual and sentinel-2A data. *European Journal of Remote Sensing*, *50*(1), 29–46. doi:10.1080/22797254.2017.1274573

Kupkova, L., & Potuckova, M. (2018). Forest cover and disturbance changes, and their driving forces: A case study in the Ore Mts., Czechia, heavily affected by anthropogenic acidic pollution in the second half of the 20th century. *Environmental Research Letters*, *13*, 095008. doi:10.1088/1748-9326/aadd2c

Lastovicka, J., Hladky, R., Staych, P., & Holman, L. (2017). Evaluation of forest disturbances in the Low Tatras National Park using time series of satellite images. In *17th International Multidisciplinary Scientific GeoConference SGEM 2017 (pp. 80-100), Albena, Bulgaria.*

Mei, A., Bassani, C., Fontinovo, G., Salvatori, R., & Allegrini, A. (2016). The use of suitable pseudo-invariant targets for MIVIS data calibration by the empirical line method. *ISPRS Journal of*

Photogrammetry and Remote Sensing, *114*, 102–114. doi:10.1016/j.isprsjprs.2016.01.016

Musilova, R. (2012). *Vyuziti dat DPZ pro hodnoceni aktualniho stavu a vyvoje smrkovych porostu v Krkonosich* (Master thesis). Faculty of Science, Charles university. Retrieved from https://is.cuni.cz/webapps/zzp/detail/119490

Neigh, C., Bolton, D., Diabate, M., Williams, J., & Carvalhais, N. (2014). An automated approach to map the history of forest disturbance from insect mortality and harvest with Landsat time-series data. *Remote Sensing*, *6*, 2782–2808. doi:10.3390/rs6042782

Polak, P., & Saxa, A. (2005). *Priaznivy stav biotopov a druhov europskeho vyznamu*. Banska Bystrica: Statna ochrana prirody SR.

Potapov, P.V., Turubanova, S.A., Tyukavina, A., Krylov, A.M., McCarty, J.L., Radeloff, V.C., & Hansen, M.C. (2015). Eastern Europe's forest cover dynamics from 1985 to 2012 quantified from the full Landsat archive. *Remote Sensing of Environment*, *159*, 28–43. doi:10.1016/j.rse.2014.11.027

Rahman, M.M., Hay, G.J., Couloigner, I., Hemachandran, B., & Bailin, J. (2015). A comparison of four relative radiometric normalization (RRN) techniques for mosaicing H-res multi-temporal thermal infrared (TIR) flight-lines of a complex urban scene. *ISPRS Journal of Photogrammetry and Remote Sensing*, *106*, 82–94. doi:10.1016/j.isprsjprs.2015.05.002

Rouse, J.W., Hass, R.H., Schell, J.A., & Deering, D.W. (1973). Monitoring vegetation systems in the great plains with ERTS. In *Third ERTS Symposium, NASA* (Vol. 1, pp. 309–317). Retrieved from https://doi.org/citeulike-article-id:12009708

Roy, D.P., Wulder, M.A., Loveland, T.R., Woodcock, C.E., Allen, R.G., Anderson, M.C., … Zhu, Z. (2014). Landsat-8: Science and product vision for terrestrial global change research. *Remote Sensing of Environment*, *145*, 154–172. doi:10.1016/j.rse.2014.02.001

Roy, D.P., Zhang, H.K., Ju, J., Gomez-Dans, J.L., Lewis, P.E., Schaaf, C.B., … Kovalskyy, V. (2016). A general method to normalize Landsat reflectance data to nadir BRDF adjusted reflectance. *Remote Sensing of Environment*, *176*, 255–271. doi:10.1016/j.rse.2016.01.023

Schroeder, T.A., Cohen, W.B., Song, C., Canty, M.J., & Yang, Z. (2006). Radiometric correction of multi-temporal Landsat data for characterization of early successional forest patterns in western Oregon. *Remote Sensing of Environment*, *103*(1), 16–26. doi:10.1016/j.rse.2006.03.008

Sitkova, Z., & Pavlenda, P. (eds). (2017). *Dlhodoby ekologicky vyskum a monitoring lesov: sucasne poznatky a vyzvy do buducnosti*. Zvolen: Narodne lesnicke centrum – Lesnicky vyskumny ustav Zvolen.

S-NAPANT. (2007). *Narodny park Nizke Tatry - prirodne hodnoty, historia, sucasny stav ochrany uzemia*. Banska Bystrica: Sprava NP Nizke Tatry.

S-NAPANT Report. (2004). *Predbezna sprava o dosledkoch veternej smrste z 19. 11.2004 na chranene uzemia a chranene druhy v uzemnej posobnosti Spravy Narodneho parku Nizke Tatry a moznosti eliminacie jej dosledkov*. Banska Bystrica: Sprava NP Nizke Tatry.

S-NAPANT Report. (2008). *Kratke zhodnotenie sucasneho stavu populacie podkorneho hmyzu na uzemi Narodneho parku Nize Tatry a jeho ochranneho pasma*. Banska Bystrica: Sprava NP Nizke Tatry, p. 11.

Song, C., Woodcock, C.E., Seto, K.C., Lenney, M.P., & Macomber, S.A. (2001). Classification and change detection using Landsat TM data: When and how to correct atmospheric effects? *Remote Sensing of Environment*, *75*(2), 230–244. doi:10.1016/S0034-4257(00)00169-3

Sovdat, B., Kadunc, M., Batic, M., & Milcinski, G. (2019). Natural color representation of Sentinel-2 data. *Remote Sensing of Environment*, *225*(September2017), 392–402. doi:10.1016/j.rse.2019.01.036

Syariz, M.A., Lin, B.Y., Denaro, L.G., Jaelani, L.M., Van Nguyen, M., & Lin, C.H. (2019). Spectral-consistent relative radiometric normalization for multitemporal Landsat 8 imagery. *ISPRS Journal of Photogrammetry and Remote Sensing*, *147*, 56–64. doi:10.1016/j.isprsjprs.2018.11.007

Vladovic, J. (2003). *Oblastne vychodiska a principy hodnotenia drevinoveho zlozenia a ekologickej stability lesov Slovenska, Lesnicke studie 57/2003, vydavatelstvo Priroda s.r.o*. Zvolen: Bratislava (pre Lesnicky vyskumny ustav. ISSBN 80- 07-01285-0.

Vladovic, J. (2011). *Struktura a diverzita lesnych ekosystemov na Slovensku*, 252.

Vogeler, J.C., Braaten, J.D., Slesak, R.A., & Falkowski, M.J. (2018). Extracting the full value of the Landsat archive: Inter-sensor harmonization for the mapping of Minnesota forest canopy cover (1973–2015). *Remote Sensing of Environment*, *209*, 363–374. doi:10.1016/j.rse.2018.02.046

Vogelmann, J.E., Xian, G., Homer, C., & Tolk, B. (2012). Monitoring gradual ecosystem change using Landsat time series analyses: Case studies in selected forest and rangeland ecosystems. *Remote Sensing of Environment*, *122*, 92–105. doi:10.1016/j.rse.2011.06.027

Vuolo, F., Mattiuzzi, M., & Atzberger, C. (2015). Comparison of the Landsat Surface Reflectance Climate Data Record (CDR) and manually atmospherically corrected data in a semi-arid European study area. *International Journal of Applied Earth Observation and Geoinformation*, *42*, 1–10. doi:10.1016/j.jag.2015.05.003

Wang, J., Sammis, T.W., Gutschick, V.P., Gebremichael, M., Dennis, S.O., & Harrison, R.E. (2010). Review of satellite remote sensing use in forest health studies. *The Open Geography Journal*, *3*(1), 28–42. doi:10.2174/1874923201003010028

Wulder, M.A., Masek, J.G., Cohen, W.B., Loveland, T.R., & Woodcock, C.E. (2012). Opening the archive: How free data has enabled the science and monitoring promise of Landsat. *Remote Sensing of Environment*, *122*, 2–10. doi:10.1016/j.rse.2012.01.010

Wulder, M.A., White, J.C., Loveland, T.R., Woodcock, C.E., Belward, A.S., Cohen, W.B., … Roy, D.P. (2016). The global Landsat archive: Status, consolidation, and direction. *Remote Sensing of Environment*, *185*, 271–283. doi:10.1016/j.rse.2015.11.032

Xie, Z., Phinn, S.R., Game, E.T., Pannell, D.J., Hobbs, R.J., Briggs, P. R., & McDonald-Madden, E. (2019). Using Landsat observations (1988–2017) and google earth engine to detect vegetation cover changes in rangelands - A first step towards identifying degraded lands for conservation. *Remote Sensing of Environment*, *232* (July), 111317. doi:10.1016/j.rse.2019.111317

Yang, X., & Lo, C.P. (2000). Relative radiometric normalization performance for change detection from multi-date satellite images. *Photogrammetric Engineering and Remote Sensing*, *66* (8), 967–980. doi:10.1016/j.fertnstert.2005.08.009

Yang, Y., Erskine, P.D., Lechner, A.M., Mulligan, D., Zhang, S., & Wang, Z. (2018). Detecting the dynamics of vegetation disturbance and recovery in surface mining area via Landsat imagery and LandTrendr algorithm. *Journal of Cleaner Production*, *178*, 353–362. doi:10.1016/j.jclepro.2018.01.050

Zemek, F., Cudlin, P., Bohac, J., Moravec, I., & Herman, M. (2003). Semi-natural forested landscape under a bark beetle

outbreak: A case study of the Bohemian Forest (Czech Republic). *Landscape Research*, *28*(3), 279–292. doi:10.1080/01426390306522

Zhu, Z., Wang, S., & Woodcock, C.E. (2015). Improvement and expansion of the Fmask algorithm: Cloud, cloud shadow, and snow detection for Landsats 4–7, 8, and Sentinel 2 images. *Remote Sensing of Environment*, *159*, 269–277. doi:10.1016/j.rse.2014.12.014

Zhu, Z., & Woodcock, C.E. (2012). Object-based cloud and cloud shadow detection in Landsat imagery. *Remote Sensing of Environment*, *118*, 83–94. doi:10.1016/j.rse.2011.10.028

Zhu, Z., & Woodcock, C.E. (2014). Continuous change detection and classification of land cover using all available Landsat data. *Remote Sensing of Environment*, *144*, 152–171. doi:10.1016/j.rse.2014.01.011